ENDURANCE CONSULTING PTY LTD

Bridge over Hawkesbury River at Windsor
Load Testing

Test Report

Prepared For:

NSW Roads and Traffic Authority

June 2011

Endurance Consulting Pty Ltd **ABN 94 123 696 588**

Suite G3, 64 Talavera Rd
MACQUARIE PARK, NSW 2113
Australia

T: (02) 9878 8940

F: (02) 9878 8941

W: www.endcon.com.au

Document Information

Title:	Bridge over Hawkesbury River at Windsor Load Testing - Test Report
Document:	E208R1
Author:	B McInnes
Consultants:	B McInnes, B Harris
Client:	NSW Roads and Traffic Authority
Client Contact:	Peter Ton
Client Reference:	O/N 4510276450

Revision/Checking History

Rev. No.	Description	Author	Reviewer	Approved	Date
0	Issued to client	BM	BH		24/06/11

Table of Contents

List of Figures

1. Introduction

1.1 General

Endurance Consulting was engaged by the NSW Roads and Traffic Authority (RTA) to provide structural measurements of Windsor Bridge over Hawkesbury River at Windsor. Performance load testing (static testing) and measurement of ambient traffic (dynamic testing) for a minimum period of 6 months is required. This document outlines the installation and presents the results of load testing.

1.2 Bridge Description

The Reinforced Concrete (RC) Beam Bridge consists of eleven spans and was built in 1931. 10 sets of 3’6” diameter wrought iron piers extend to the river bed. Figure 1-1 shows the instrumented piers.

1.3 Requirements

Measurements at piers 4, 5, 6 and 7 are required for the analysis of static load testing and ambient traffic monitoring. Bending strain in the piers is of concern, so at each location a strain gauge installed on both the south and north side allows bending to be resolved. A sampling frequency above 200 Hz is expected sufficient to capture bridge dynamic events.

Figure 1-1. RTA Bridge – Windsor Bridge Piers

2. Instrumentation

2.1 Instrumentation Layout

Figure 2-1 below shows the numbering conventions for the installed strain gauges at piers 4 to 7.

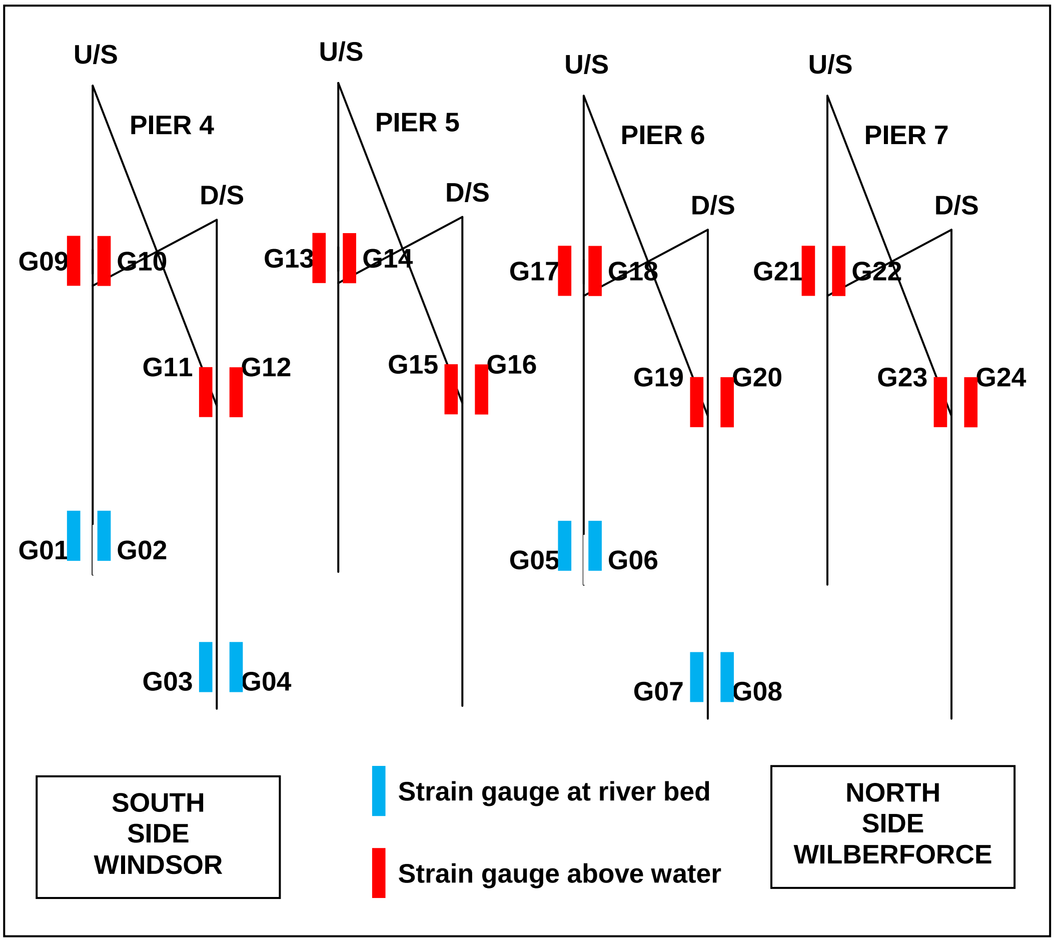

Figure 2-1. Instrumentation Layout

Table 2-1 below further indicates the positioning of the strain gauges.

Table 2-1. Sensor Locations

Transducer	Name	Pier	Side / Depth*
Demountable Strain Gauge at River Bed	G01	P4 U/S	S/S 7.49m
	G02	P4 U/S	N/S 7.49m
	G03	P4 D/S	S/S 6.72m
	G04	P4 D/S	N/S 6.72m
	G05	P6 U/S	S/S 7.14m
	G06	P6 U/S	N/S 7.14m
	G07	P6 D/S	S/S 6.45m
	G08	P6 D/S	N/S 6.45m
Foil Strain Gauge	G09	P4 U/S	S/S 1.65m
	G10	P4 U/S	N/S 1.65m
	G11	P4 D/S	S/S 1.65m
	G12	P4 D/S	N/S 1.65m
	G13	P5 U/S	S/S 1.65m
	G14	P5 U/S	N/S 1.65m
	G15	P5 D/S	S/S 1.65m
	G16	P5 D/S	N/S 1.65m
	G17	P6 U/S	S/S 1.65m
	G18	P6 U/S	N/S 1.65m
	G19	P6 D/S	S/S 1.65m
	G20	P6 D/S	N/S 1.65m
	G21	P7 U/S	S/S 1.65m
	G22	P7 U/S	N/S 1.65m
	G23	P7 D/S	S/S 1.65m
	G24**	P7 D/S	N/S 1.65m
Displacement	DDT01**	P4 D/S	kerb

U/S – Upstream, D/S – Downstream, S/S – South Side, N/S – North Side

**All depth measurements are taken from the underside flange of the bolted pier connections*

***G24 was replaced with DDT01 during testing only*

2.2 Data Acquisition Hardware

National Instruments hardware acquired all channels at a sampling frequency of 2000Hz. This data was then re-sampled to 200Hz employing appropriate anti-aliasing filters. Labview software was used for data processing. Figure 5-1 shows the location of the hardware.

2.3 Expansion Joint Transducer

For the period of the static testing a dynamic displacement transducer was installed at the Pier 4 expansion joint. The sensor was mounted on the downstream kerb as shown in photo Figure 5-4.

2.4 Strain Gauges

The following strain gauges were used to obtain the required measurements:

- Strap-On Strain Gauges – 8 off, 300mm gauge length, 350 ohm full bridge strain sensing elements fastened between two 50x5mm flat bar rings. Installed by CDS Pty Ltd. Straps were initially manufactured to a circumference of 3730mm whereas the actual pier circumference was 3370mm. On-site modifications took place resulting in the strain elements now aligning 180mm to the outboard side on the centreline.
- Foil Strain Gauges – 16 off, TML WFCA-6 120 ohm half bridge gauges.

Figures 2-2 and 2-3 below show two types of strain gauges

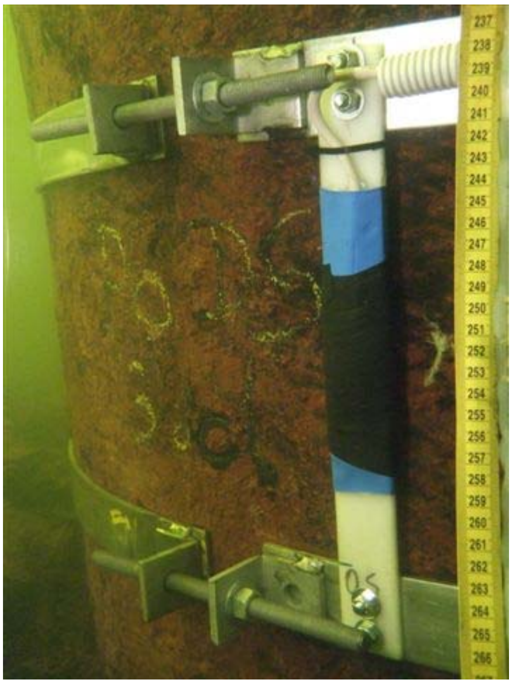

Figure 2-2. Instrumentation – Strap-On Gauge

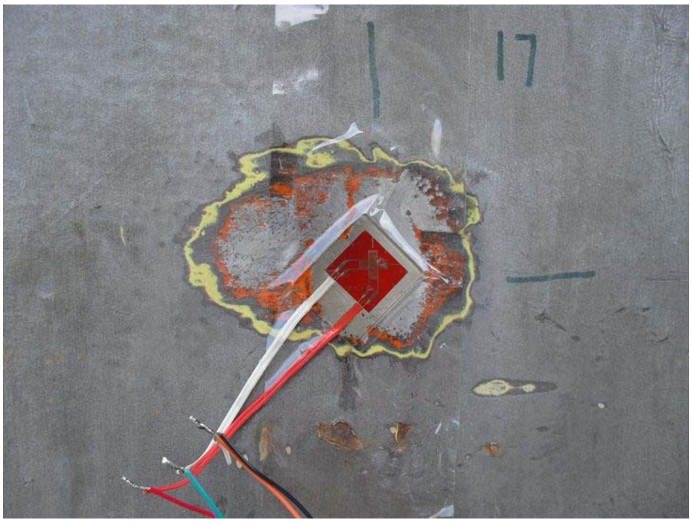

Figure 2-3. Instrumentation – Foil Strain Gauge

3. Static Test Results

3.1 Test Conditions

Planned load testing with the RTA Test Truck was carried out on the night of 8 June 2011. Normal carriageway was used for all tests. Three load levels were tested during the crawl tests as indicated in Table 3-1. Braking tests were also conducted on approach to Pier 4 and Pier 7 from both directions.

3.2 Test Vehicle and Loadings

The planned load testing was conducted by using an RTA dedicated test vehicle as shown in Figure 3-1.

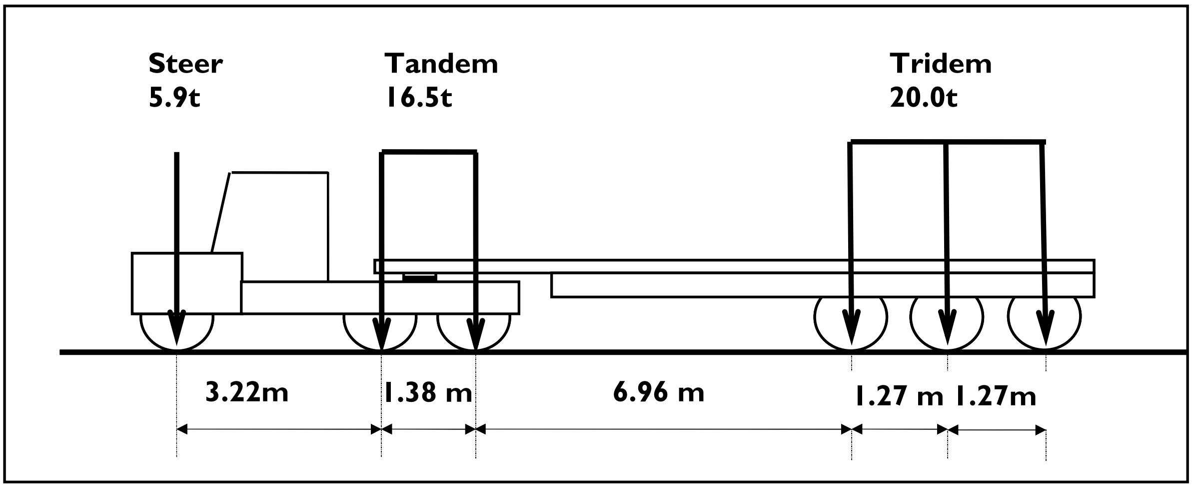

Figure 3-1. RTA Test Vehicle

The three loading levels used in performance load testing are shown in Table 3-1.

Table 3-1. Approximate Loadings

Test Truck	Load Level	Group Loads (t)			Equivalent GVM (t)
		Steer	Tandem	Tridem	
RTA	**1**	5.9	16.5	20.0	42.4
	2	5.9	16.5	25.0	47.4
	3	5.9	16.5	30.0	52.4

3.3 Results Presented

For each test the maximum strain relative to the unloaded strain has been calculated and presented in tabular form (Section 3.4). Section 3.5 displays selected example waveform (time series). Bending results for each pair of gauges are calculated as:

Bending Strain = (North Side Strain – South Side Strain) / 2

The bending strains are generally low so only the absolute maximum has been reported for each test.

3.4 Tabulated Static Test Results

Tabulated results are found in Tables:

- 3-2. Results for test with no braking
- 3-3. Results of test with braking on approach to Pier 4.
- 3-4. Results of tests with braking on approach to Pier 7.

The following abbreviations are used in the tables:

P# Pier#

US Upstream

DS Downstream

RB River Bed

AW Above Water

SS South Side

NS North Side

DDT Dynamic Displacement Transducer

Table 3-2. Non- Braking Test Results

TRIDEM LOAD LEVEL		20t	20t	20t	20t	25t	25t	30t	30t
SPEED (km/hr)		Crawl	Crawl	40	40	Crawl	Crawl	Crawl	Crawl
BRAKING		NO	NO	NO	NO	NO	NO	NO	NO
DIRECTION		South	North	South	North	South	North	South	North
TIME		10:28	01:10	11:03	11:04	11:29	11:36	11:58	12:05
Gauge #	Location	Compressive Strain (microstrain)							
G01	P4 US RB SS	2.9	9.9	4.2	10.7	3.5	11.1	3.6	12.0
G02	P4 US RB NS	2.6	6.7	3.3	8.1	3.4	7.3	3.7	8.2
G03	P4 DS RB SS	7.0	3.4	8.2	2.6	8.0	3.7	9.0	3.9
G04	P4 DS RB NS	7.5	2.9	7.6	3.1	8.6	2.4	9.9	3.3
G05	P6 US RB SS	5.8	19.4	7.3	21.3	7.0	23.0	7.4	25.6
G06	P6 US RB NS	6.9	19.8	7.3	22.2	9.1	22.7	9.6	25.4
G07	P6 DS RB SS	17.1	6.0	18.0	5.4	19.0	5.7	21.3	6.5
G08	P6 DS RB NS	23.3	8.2	23.3	7.9	26.5	7.1	29.2	8.3
G09	P4 US AW SS	6.7	15.2	6.9	17.6	7.4	16.8	8.9	18.9
G10	P4 US AW NS	6.3	15.6	6.7	18.7	6.6	19.4	7.2	22.1
G11	P4 DS AW SS	18.5	8.3	19.7	6.7	21.9	7.5	25.5	9.1
G12	P4 DS AW NS	12.6	6.6	12.0	7.0	13.9	7.6	15.5	8.3
G13	P5 US AW SS	6.9	19.6	7.7	22.3	8.8	21.7	10.1	24.5
G14	P5 US AW NS	6.5	17.6	7.6	19.9	6.1	21.7	8.0	25.0
G15	P5 DS AW SS	10.0	4.9	9.2	4.8	12.0	4.8	13.9	5.3
G16	P5 DS AW NS	16.3	6.2	15.1	5.8	13.4	7.6	18.6	8.8
G17	P6 US AW SS	7.4	17.9	8.0	19.5	7.3	19.8	10.7	22.7
G18	P6 US AW NS	6.1	15.1	6.6	14.5	6.8	18.6	7.3	21.6
G19	P6 DS AW SS	19.2	7.9	20.0	8.7	18.8	7.9	26.0	7.9
G20	P6 DS AW NS	21.4	8.0	20.2	7.4	22.5	8.8	25.2	10.8
G21	P7 US AW SS	7.8	19.7	9.0	21.4	9.8	21.6	11.1	24.7
G22	P7 US AW NS	6.0	17.5	8.1	18.4	7.0	20.7	7.7	23.6
G23	P7 DS AW SS	19.3	7.7	19.5	8.7	22.2	7.6	25.9	8.4
DDT (mm) Min	P4 DS Kerb	-0.24	-0.13	-0.27	-0.11	-0.28	-0.08	-0.26	-0.09
DDT (mm) Max	P4 DS Kerb	0.69	0.31	0.67	0.32	0.76	0.31	0.87	0.35
Bending Strain	Absolute Max	7.7	6.2	8.9	7.7	9.3	7.0	11.0	8.2

Table 3-3. Braking at Pier 4 Test Results

TRIDEM LOAD LEVEL		20t	20t	20t	20t	20t	20t	20t	20t
SPEED (km/hr)		20	20	30	30	40	40	50	50
BRAKING		@ P4	@ P4	@ P4	@ P4	@ P4	@ P4	@ P4	@ P4
DIRECTION		South	North	South	North	North	South	South	North
TIME		12:52	12:54	12:58	01:00	01:05	01:07	01:15	01:17
Gauge #	Location	Compressive Strain (microstrain)							
G01	P4 US RB SS	3.7	9.9	4.3	10.3	10.5	4.4	4.9	10.0
G02	P4 US RB NS	3.8	6.4	3.8	6.6	8.0	2.8	3.7	6.6
G03	P4 DS RB SS	7.6	3.3	8.2	3.3	2.9	8.9	9.2	2.9
G04	P4 DS RB NS	9.3	3.8	9.1	4.1	5.3	7.5	8.3	3.8
G05	P6 US RB SS	7.5	21.4	6.7	21.2	21.3	7.7	7.8	20.1
G06	P6 US RB NS	7.9	21.4	7.9	20.5	21.1	7.3	8.5	20.7
G07	P6 DS RB SS	16.9	6.1	17.0	5.8	6.2	17.4	16.7	5.8
G08	P6 DS RB NS	23.5	7.4	22.9	7.5	7.9	22.5	23.2	8.8
G09	P4 US AW SS	7.3	15.4	6.9	15.3	15.9	6.8	7.3	15.5
G10	P4 US AW NS	6.7	15.9	7.1	16.5	15.7	6.4	6.9	15.6
G11	P4 DS AW SS	20.1	8.3	19.2	8.0	8.2	20.4	19.0	7.2
G12	P4 DS AW NS	12.7	6.9	13.7	6.6	6.4	13.2	12.9	6.3
G13	P5 US AW SS	7.4	19.6	8.1	19.7	20.3	7.2	7.4	18.8
G14	P5 US AW NS	7.7	17.7	7.8	17.4	18.1	7.5	7.8	17.4
G15	P5 DS AW SS	9.9	4.8	10.1	4.4	4.7	9.0	9.2	4.6
G16	P5 DS AW NS	15.5	6.4	15.8	5.8	6.6	15.4	15.0	6.1
G17	P6 US AW SS	7.8	17.6	8.0	17.5	17.9	7.6	8.6	18.3
G18	P6 US AW NS	8.3	15.2	7.4	15.9	15.1	7.0	7.9	15.2
G19	P6 DS AW SS	19.8	7.7	20.8	7.9	7.7	19.8	19.4	8.1
G20	P6 DS AW NS	22.4	8.4	21.2	8.5	9.0	20.9	20.4	8.5
G21	P7 US AW SS	9.4	20.3	9.1	19.8	20.0	9.4	10.0	19.3
G22	P7 US AW NS	7.9	17.7	7.2	16.7	16.6	7.1	7.6	20.5
G23	P7 DS AW SS	20.6	8.9	19.0	8.8	8.2	18.8	20.4	8.0
DDT (mm) Min	P4 DS Kerb	-0.21	-0.13	-0.22	-0.10	-0.15	-0.26	-0.22	-0.10
DDT (mm) Max	P4 DS Kerb	0.67	0.30	0.64	0.29	0.28	0.60	0.61	0.29
Bending Strain	Absolute Max	8.7	6.4	8.2	6.4	6.2	8.4	8.5	7.4

Table 3-4. Braking at Pier 7 Test Results

	TRIDEM LOAD LEVEL	20t	20t	20t	20t	20t	20t	20t	20t
	SPEED (km/hr)	20	20	30	30	40	40	50	50
	BRAKING	@ P7	@ P7	@ P7	@ P7	@ P7	@ P7	@ P7	@ P7
	DIRECTION	South	North	South	North	South	North	South	North
	TIME	01:20	01:22	01:26	01:27	01:30	01:33	01:35	01:37
Gauge #	Location	Compressive Strain (microstrain)							
G01	P4 US RB SS	3.8	9.8	3.5	9.8	3.6	9.8	3.7	10.0
G02	P4 US RB NS	3.4	6.6	2.9	7.1	3.3	7.0	2.9	6.9
G03	P4 DS RB SS	7.2	2.9	7.2	2.9	7.6	2.7	7.5	3.0
G04	P4 DS RB NS	8.5	3.0	8.0	2.7	8.8	3.2	7.9	3.1
G05	P6 US RB SS	6.9	20.2	7.5	22.4	8.5	20.4	11.4	21.9
G06	P6 US RB NS	7.4	21.6	7.9	23.1	7.4	22.3	8.1	24.4
G07	P6 DS RB SS	17.3	6.3	17.5	8.1	17.7	8.6	20.4	9.2
G08	P6 DS RB NS	22.9	7.8	24.2	8.8	23.2	9.2	22.7	10.2
G09	P4 US AW SS	8.0	16.0	7.3	15.0	8.5	14.7	7.3	16.2
G10	P4 US AW NS	6.9	16.7	6.5	16.3	6.2	16.6	6.0	16.4
G11	P4 DS AW SS	22.8	8.4	21.7	7.7	23.8	7.5	21.8	7.9
G12	P4 DS AW NS	13.0	6.9	13.5	6.7	13.3	6.6	13.1	6.6
G13	P5 US AW SS	7.7	19.7	7.9	20.5	7.8	21.7	8.1	19.8
G14	P5 US AW NS	8.0	18.7	6.8	19.9	7.1	20.0	7.4	19.2
G15	P5 DS AW SS	11.0	4.7	10.6	4.6	10.4	5.6	10.5	4.5
G16	P5 DS AW NS	17.0	6.2	16.0	6.5	15.4	6.3	15.6	6.3
G17	P6 US AW SS	7.9	17.9	7.4	18.4	7.5	19.0	7.9	19.0
G18	P6 US AW NS	6.5	15.3	6.9	17.5	7.0	16.6	7.5	17.0
G19	P6 DS AW SS	20.4	7.9	18.9	8.6	18.4	9.6	19.1	8.5
G20	P6 DS AW NS	21.2	8.0	21.4	9.6	21.8	10.3	21.8	10.1
G21	P7 US AW SS	8.5	20.4	9.6	21.1	8.3	20.5	8.5	20.2
G22	P7 US AW NS	7.7	17.1	7.2	17.3	6.8	17.1	8.0	17.0
G23	P7 DS AW SS	18.8	7.3	21.0	8.0	19.4	8.0	18.6	7.4
DDT (mm) Min	P4 DS Kerb	-0.23	-0.14	-0.27	-0.22	-0.28	-0.23	-0.51	-0.27
DDT (mm) Max	P4 DS Kerb	0.67	0.30	0.66	0.27	0.70	0.29	0.64	0.31
Bending Strain	Absolute Max	9.5	6.7	9.1	6.8	10.8	7.2	9.1	6.9

3.5 Results Discussion

The following observations can be made from the test period and the presented results:

- Bending strain is not the dominant strain in the piers. All strain gauges go into compression under loading in all test instances.
- The braking tests did not increase bending strain results or expansion gap openings.
- The expansion gap opening is due to the method of measurement being sensitive to the flexure of the spans. Braking tests did not increase the values so it considered that they did not contribute to the expansion joint opening.
- Pier 4 river bed gauges on both upstream and downstream display less axial compression then the corresponding above water gauges.
- Pier 6 river bed gauges correlate well with the results from the above water gauges.

3.6 Graphical Static Test Results

Figures 3-2 to 3-9 graphically represent a sample of the above data. Plots are shown for tests at times 10:28PM and 11:03PM. (Negative indicates compressive strain).

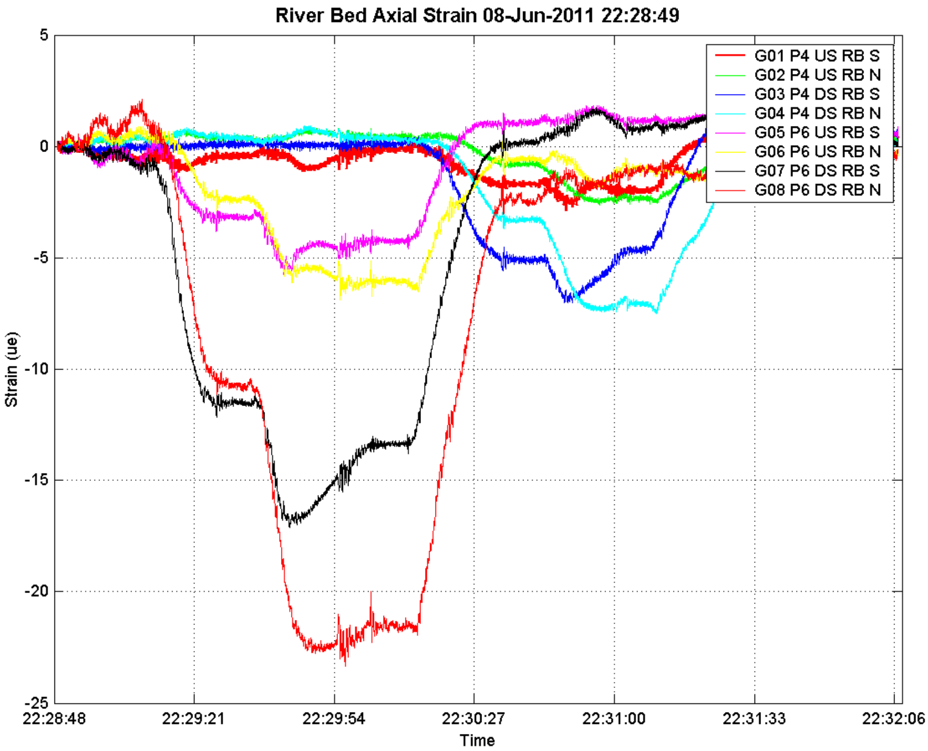

Figure 3-2. 10:28PM Axial Strain (RB)

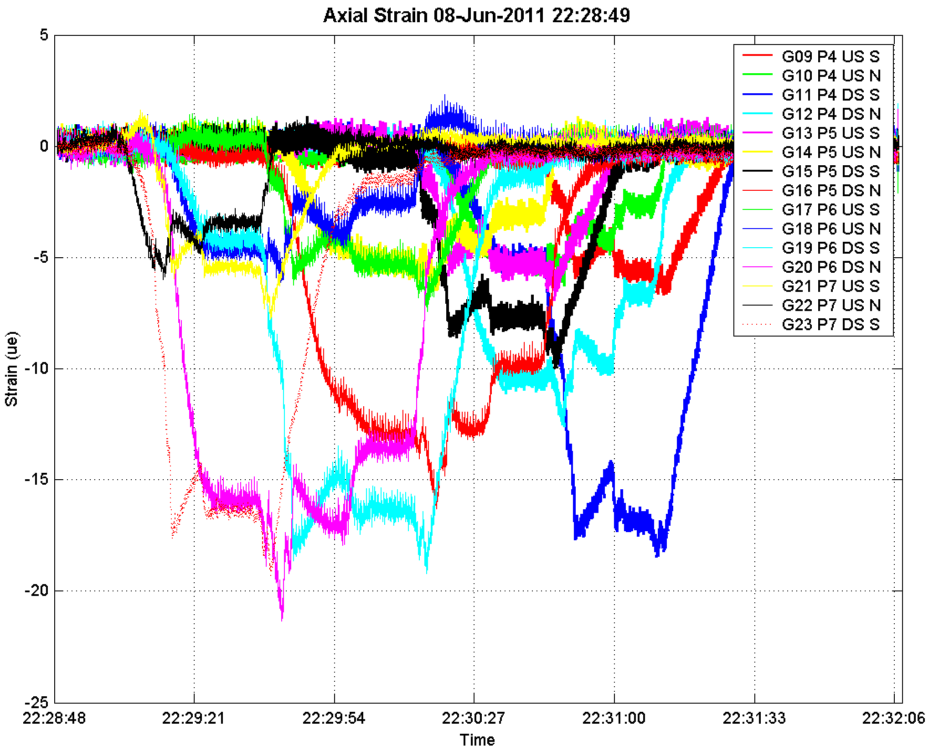

Figure 3-3. 10:28PM Axial Strain (AW)

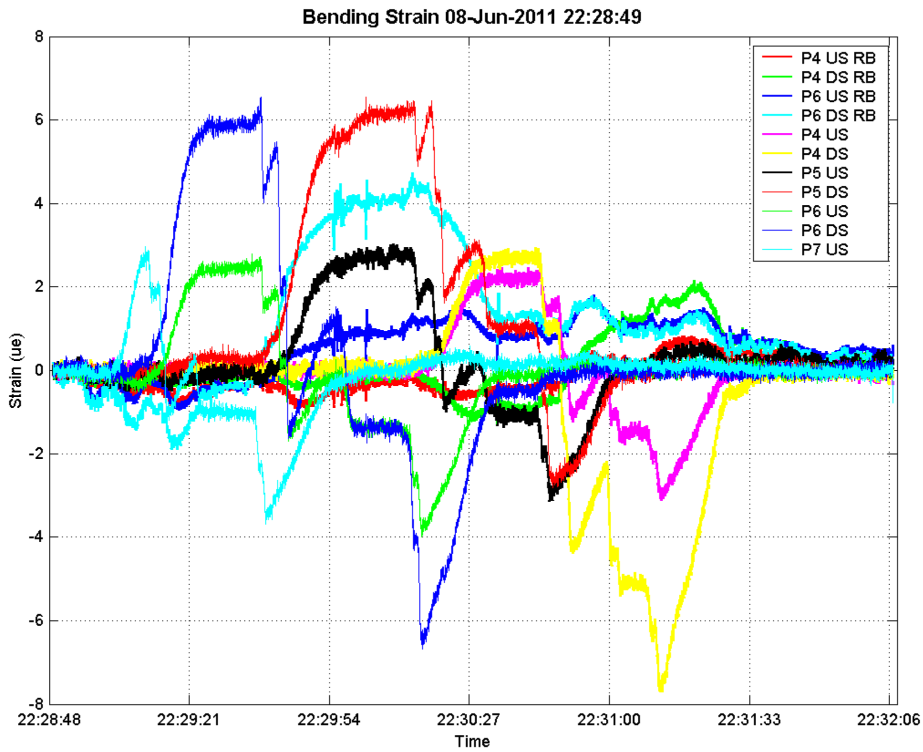

Figure 3-4. 10:28PM Bending Strain

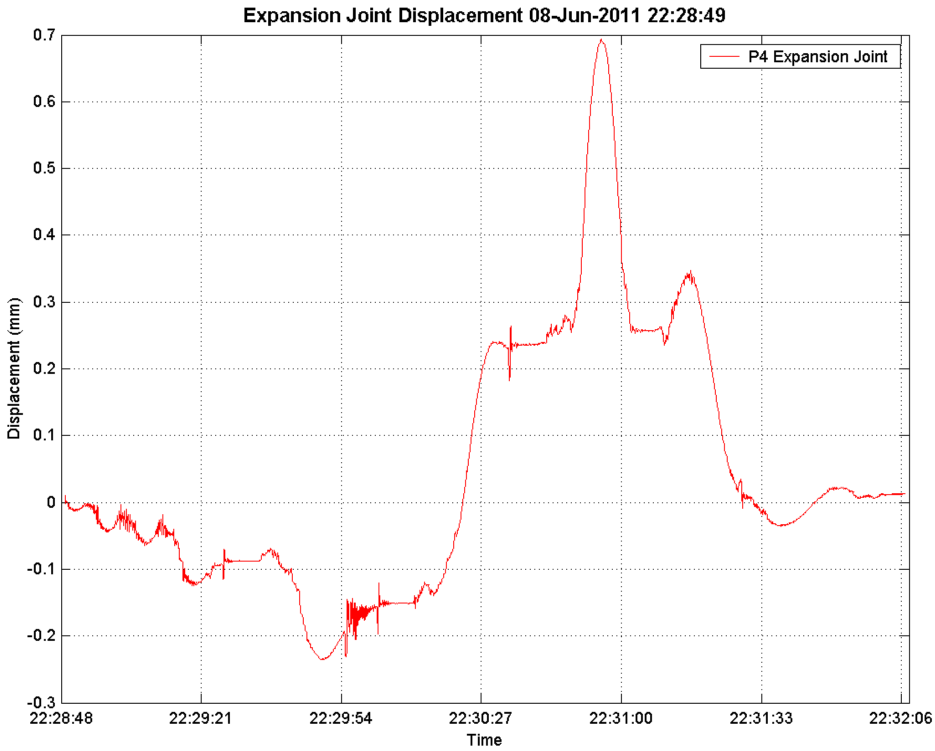

Figure 3-5. 10:28PM Expansion Joint

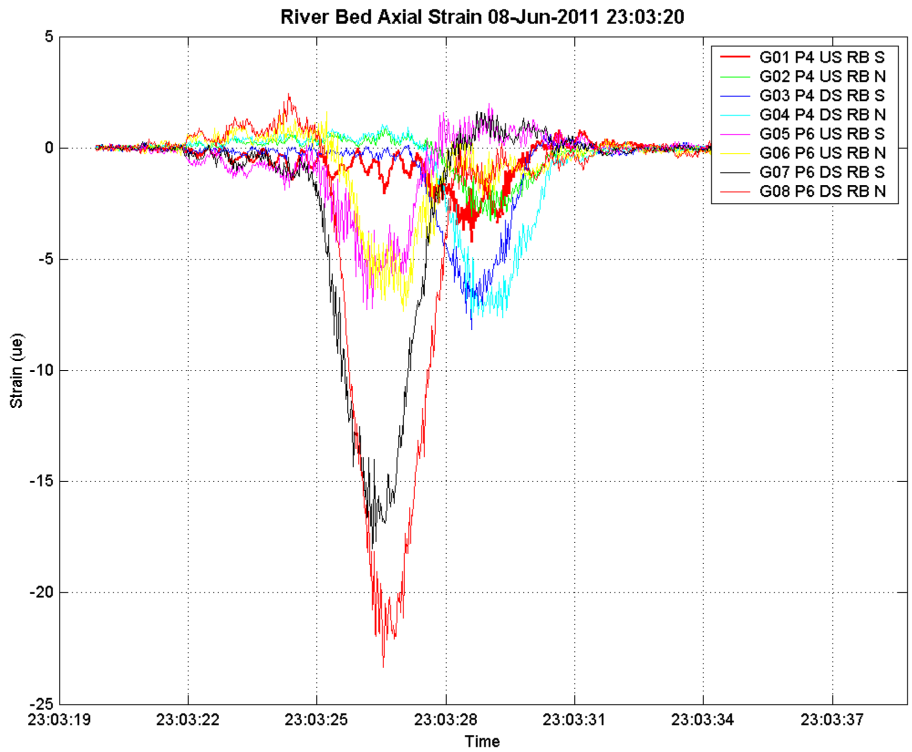

Figure 3-6. 11:03PM Axial Strain (RB)

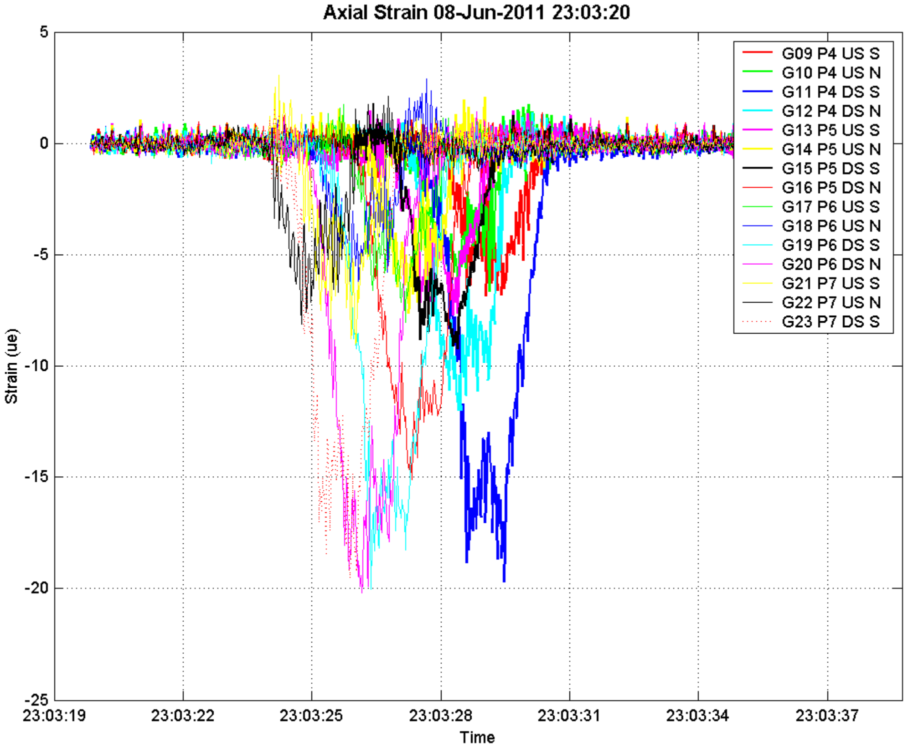

Figure 3-7. 11:03PM Axial Strain (AW)

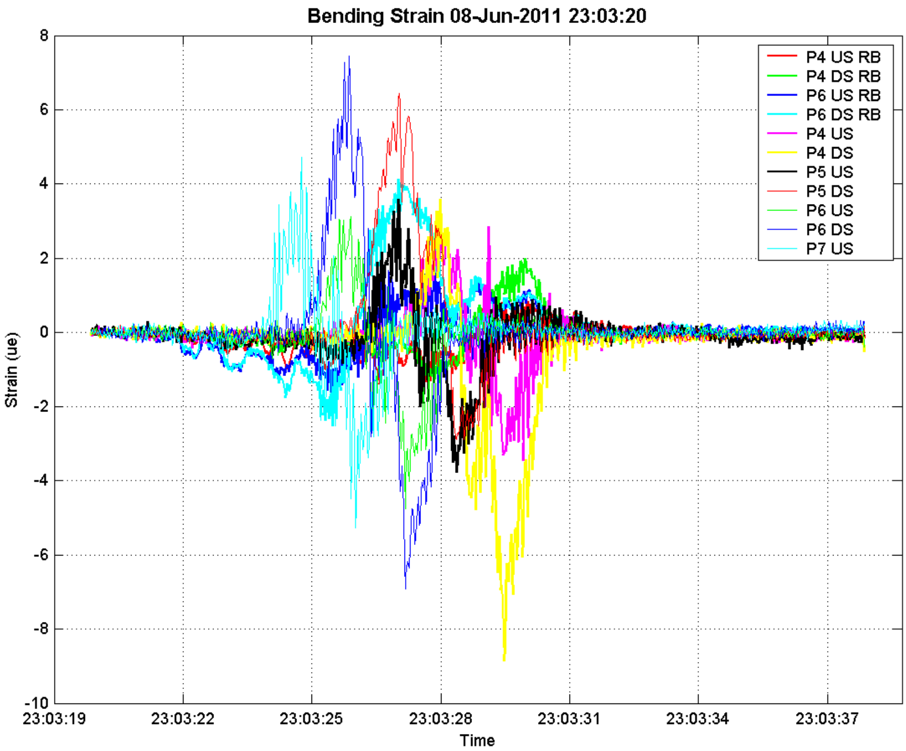

Figure 3-8. 11:03PM Bending Strain

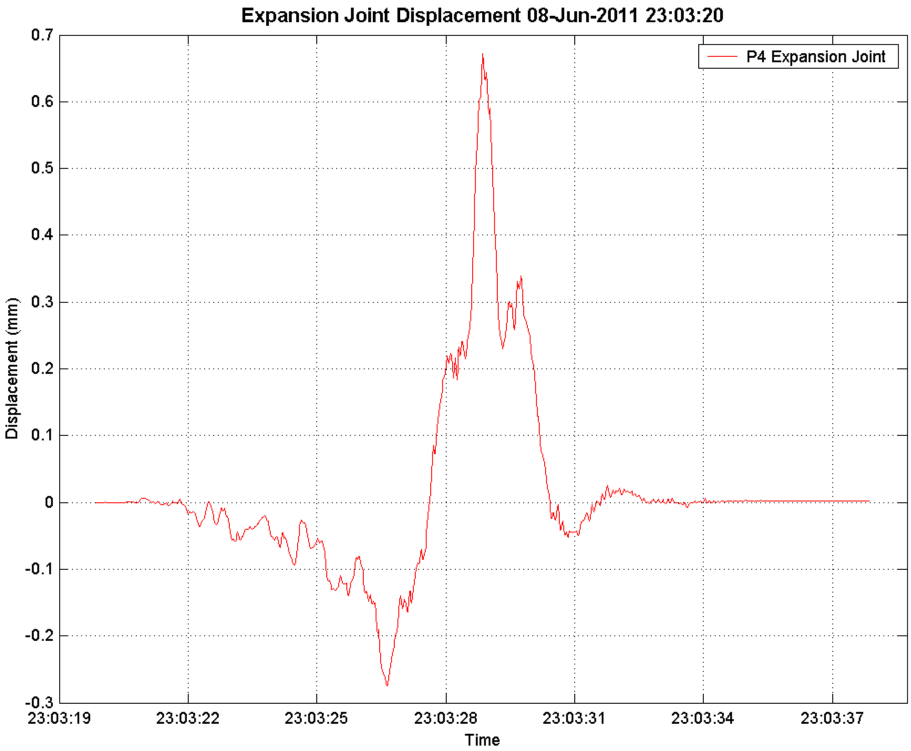

Figure 3-9. 11:03PM Expansion Joint

4. Dynamic Test Results (Monitoring of Ambient Traffic)

4.1 Test Overview

Installation of continuous power via solar panels was completed on 17 June 2011 and dynamic testing of ambient traffic was initiated that day. Data from 17 to 24 June is presented in this section. A 40 second period of time series data is acquired to enable full post-processing.

4.2 Results Processing

Traffic events which cause strain deviations above a set point have been logged and are presented in Sections 4.3. The nominal trigger set points used were G18 - 15 $\mu\varepsilon$, and G20 -20$\mu\varepsilon$ for axial strains. Waveforms of peak events were viewed to confirm that the event fitted the expected profile and was indeed a vehicle.

Additional data can be viewed on the website www.endcon.com.au/clients/nswrta/bn415 .

4.3 Scatter Plots

Figure 4-1 to 4-12 show axial strain scatter plots for each pier upstream and downstream with a red line mark indicating the load level 1 test at 40kph results from Section 3.3. Figure 4-13 to 4-24 show bending strain scatter plots for each pier upstream and downstream.

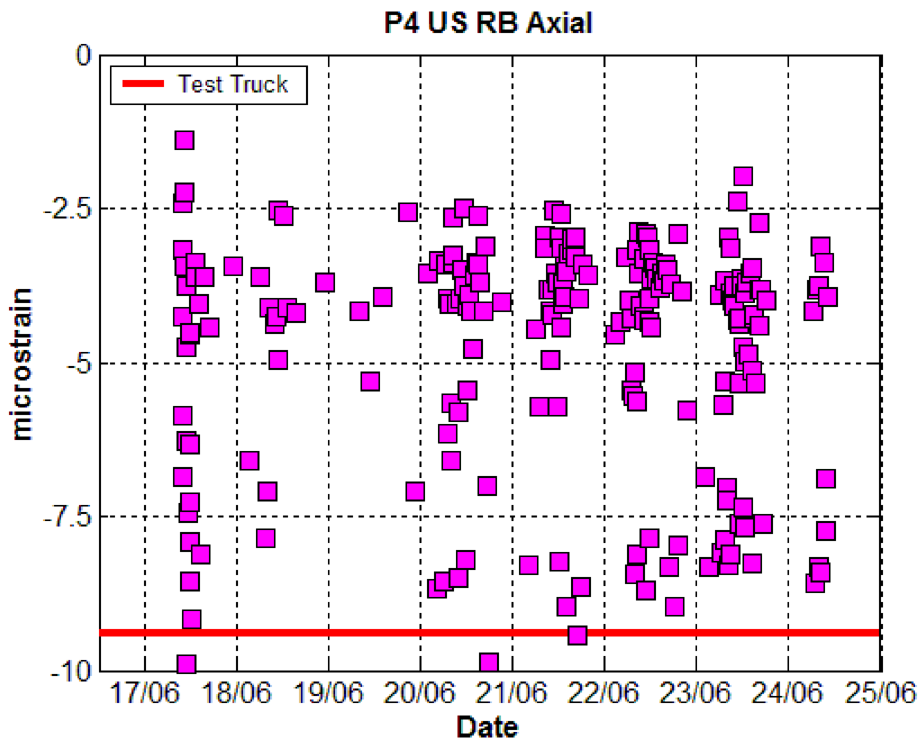

Figure 4-1. Scatter Plot - Pier 4 Upstream Axial Strain (RB)

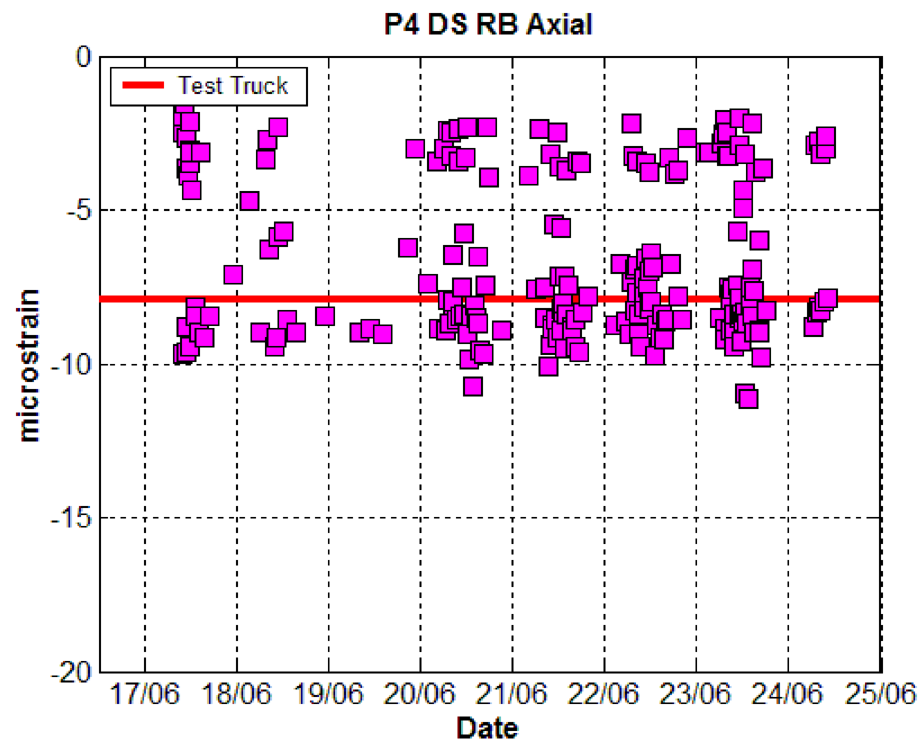

Figure 4-2. Scatter Plot - Pier 4 Downstream Axial Strain (RB)

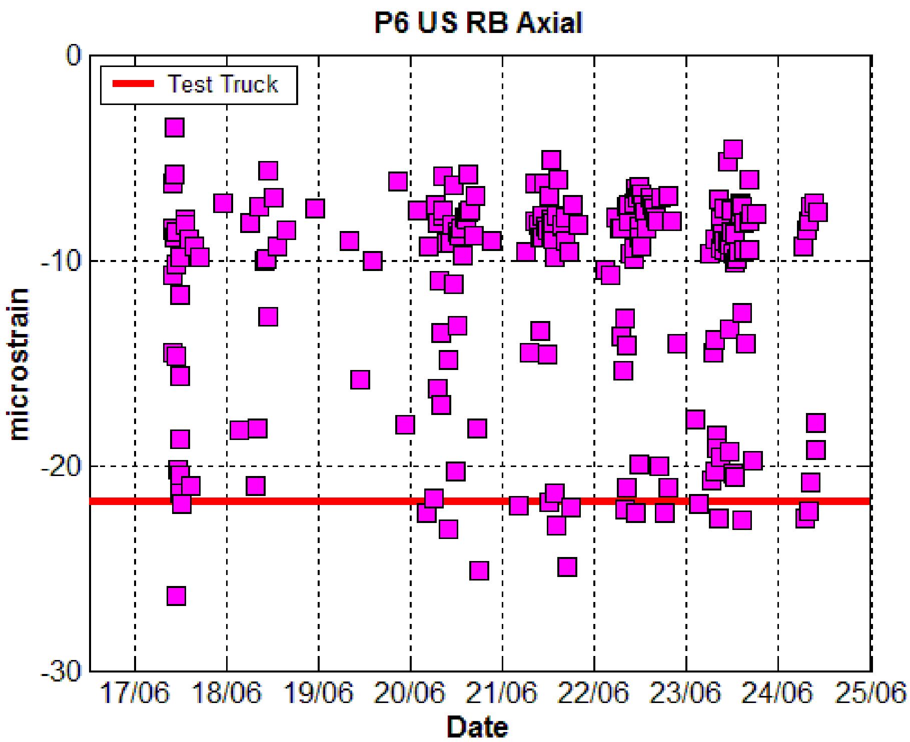

Figure 4-3. Scatter Plot - Pier 6 Upstream Axial Strain (RB)

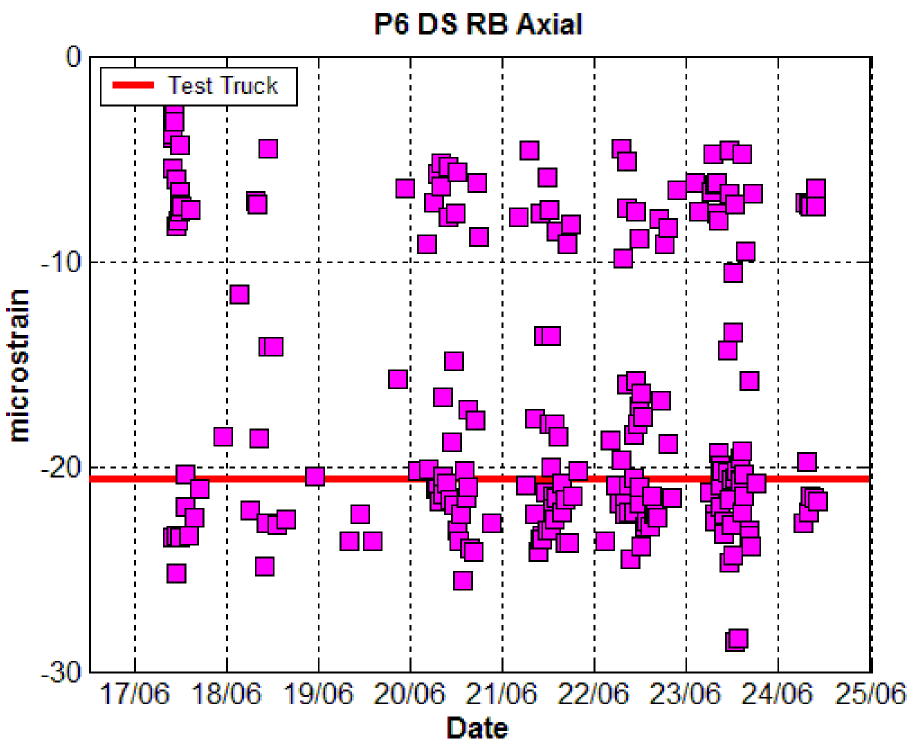

Figure 4-4. Scatter Plot - Pier 6 Downstream Axial Strain (RB)

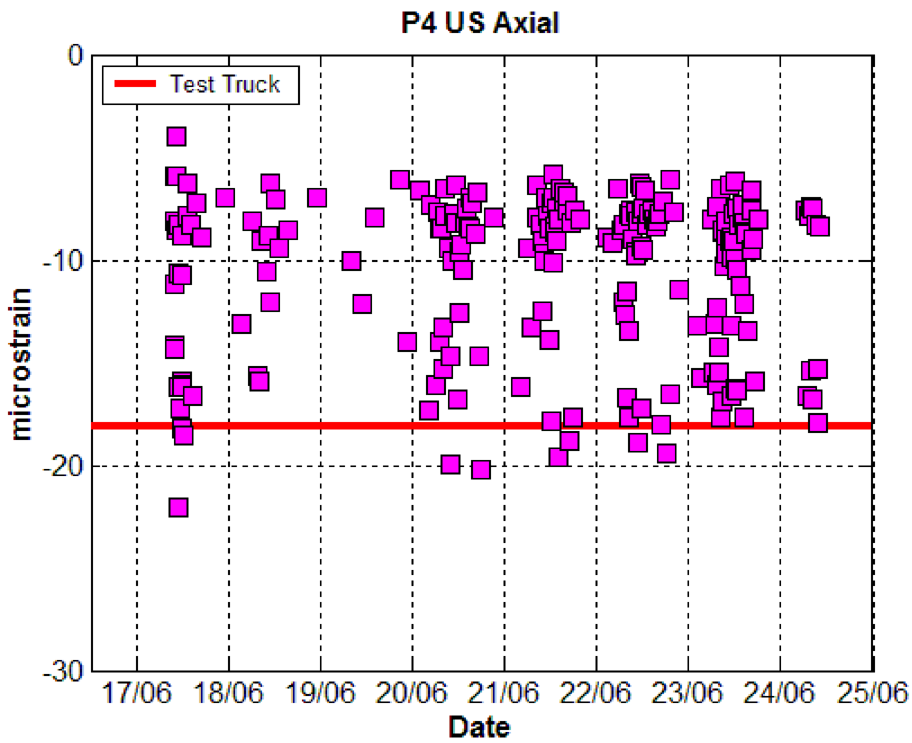

Figure 4-5. Scatter Plot - Pier 4 Upstream Axial Strain

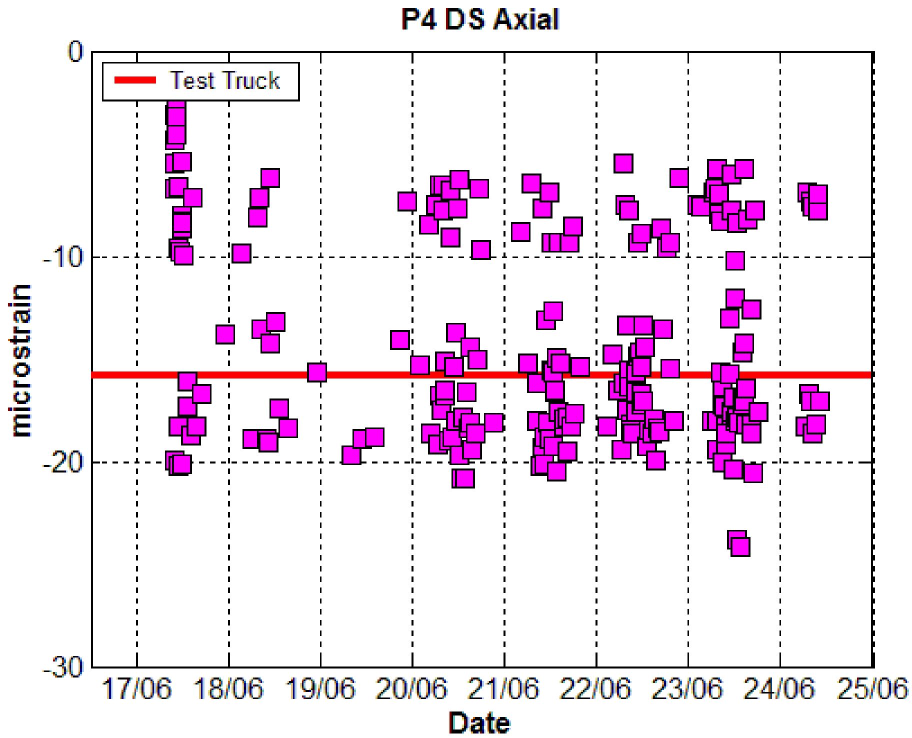

Figure 4-6. Scatter Plot - Pier 4 Downstream Axial Strain

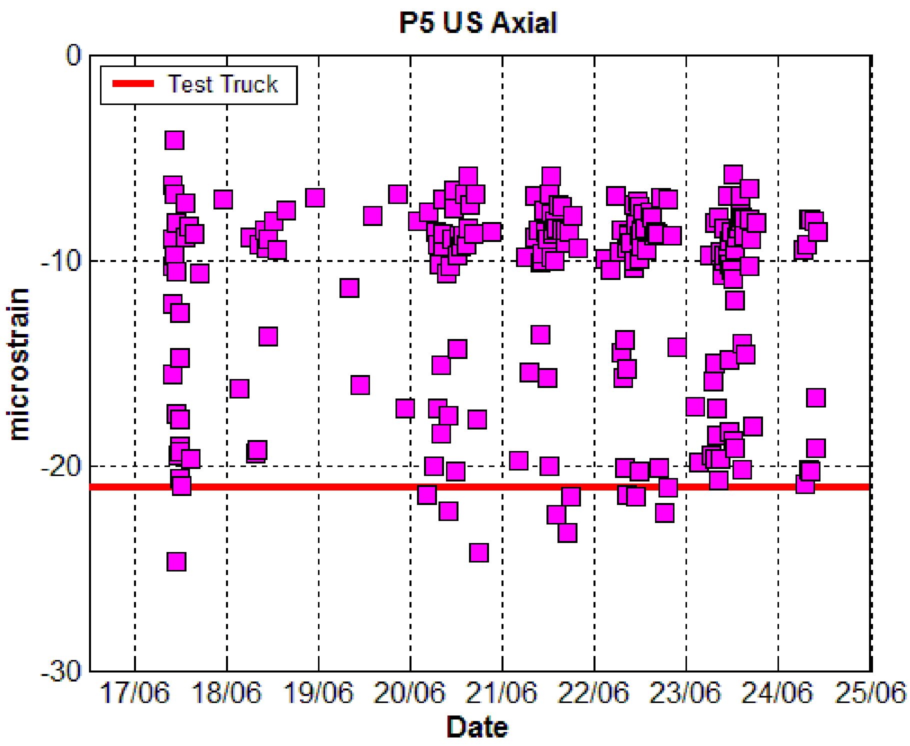

Figure 4-7. Scatter Plot - Pier 5 Upstream Axial Strain

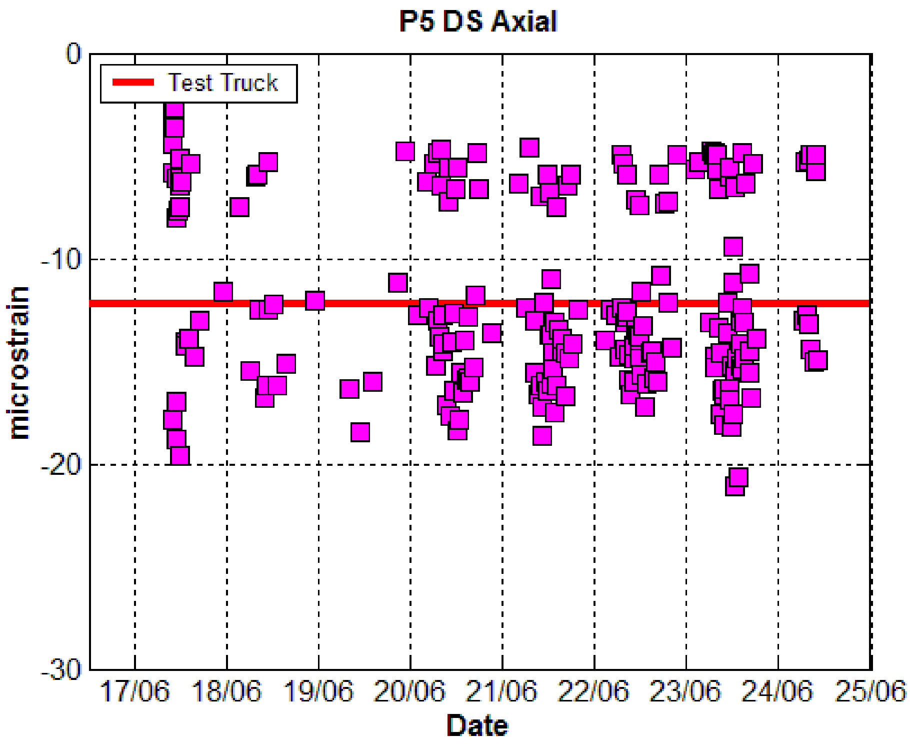

Figure 4-8. Scatter Plot - Pier 5 Downstream Axial Strain

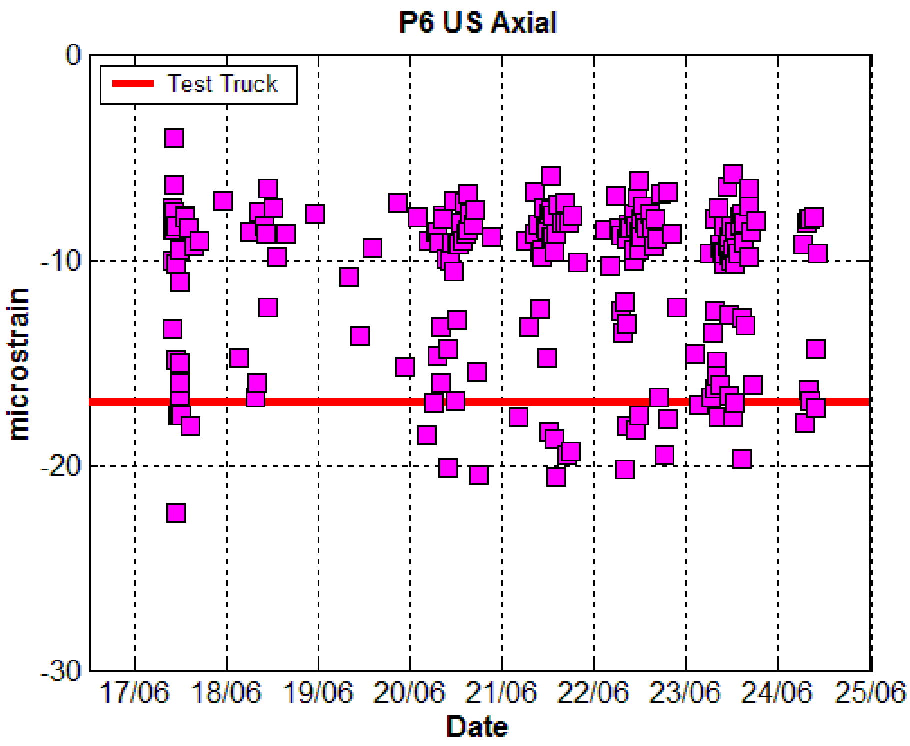

Figure 4-9. Scatter Plot - Pier 6 Upstream Axial Strain

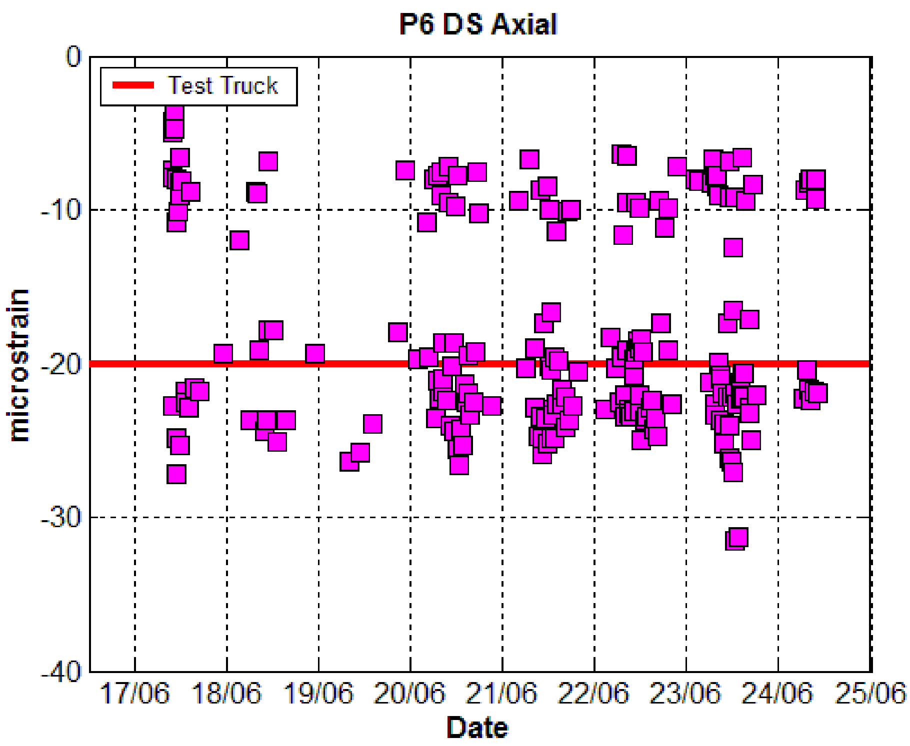

Figure 4-10. Scatter Plot - Pier 6 Downstream Axial Strain

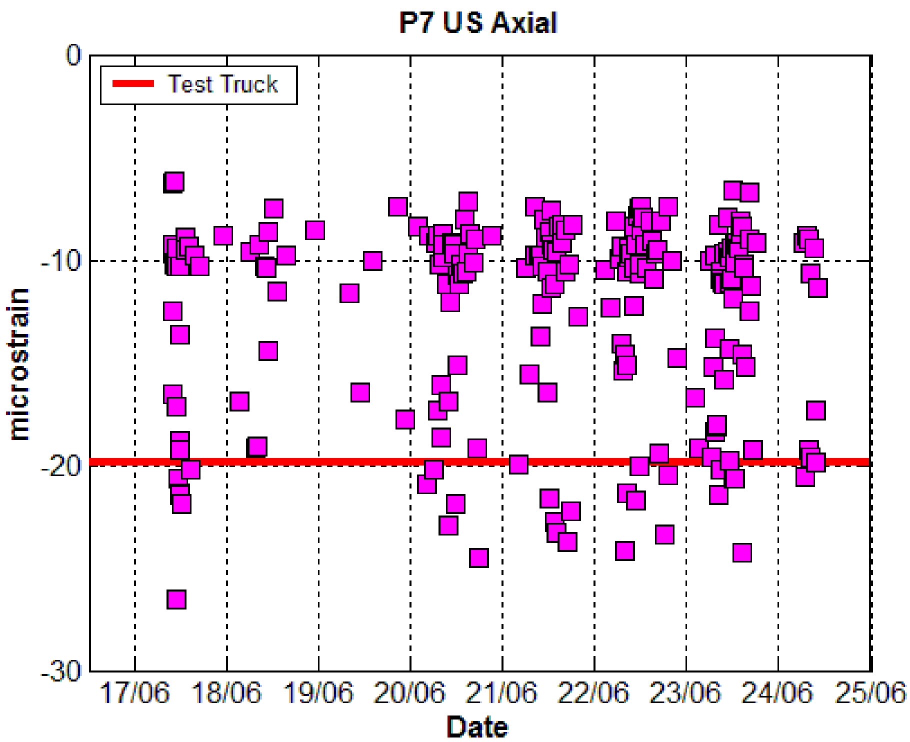

Figure 4-11. Scatter Plot - Pier 7 Upstream Axial Strain

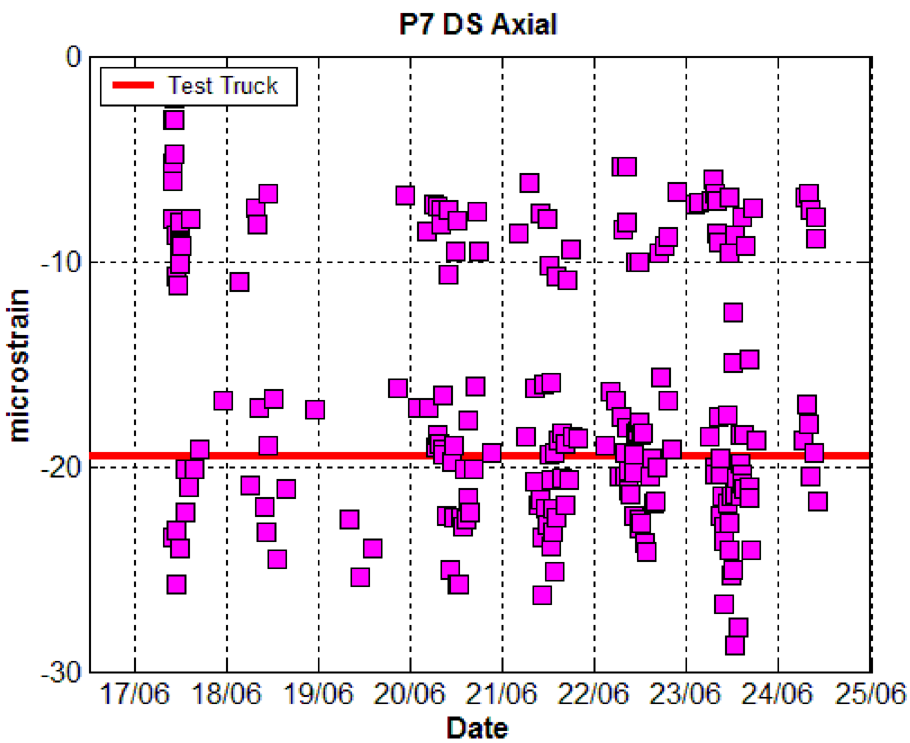

Figure 4-12. Scatter Plot - Pier 7 Downstream Axial Strain

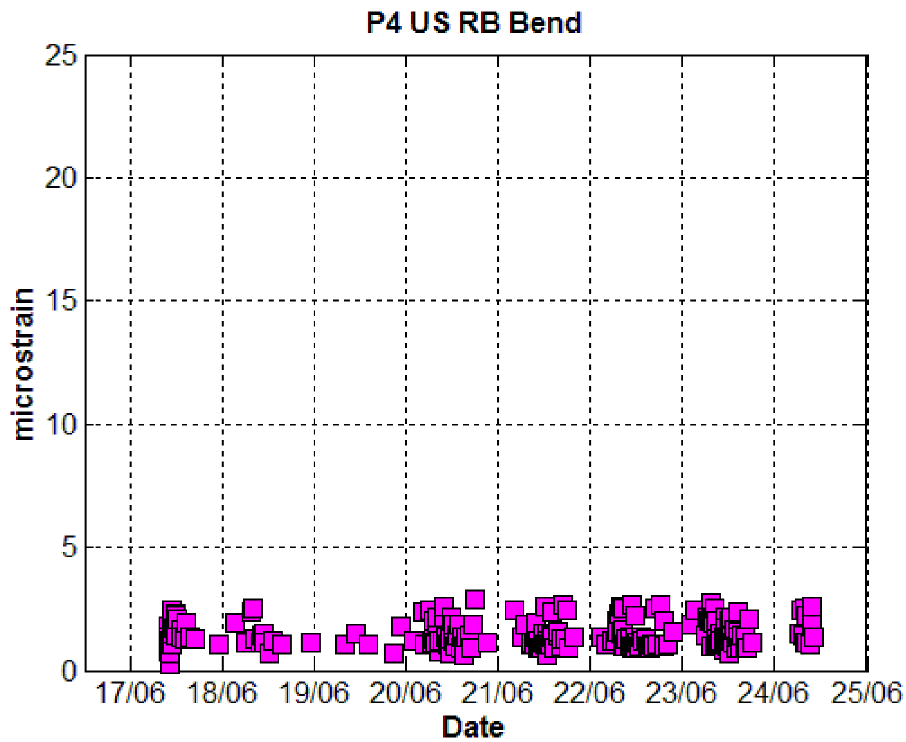

Figure 4-13. Scatter Plot - Pier 4 Upstream Bending Strain (RB)

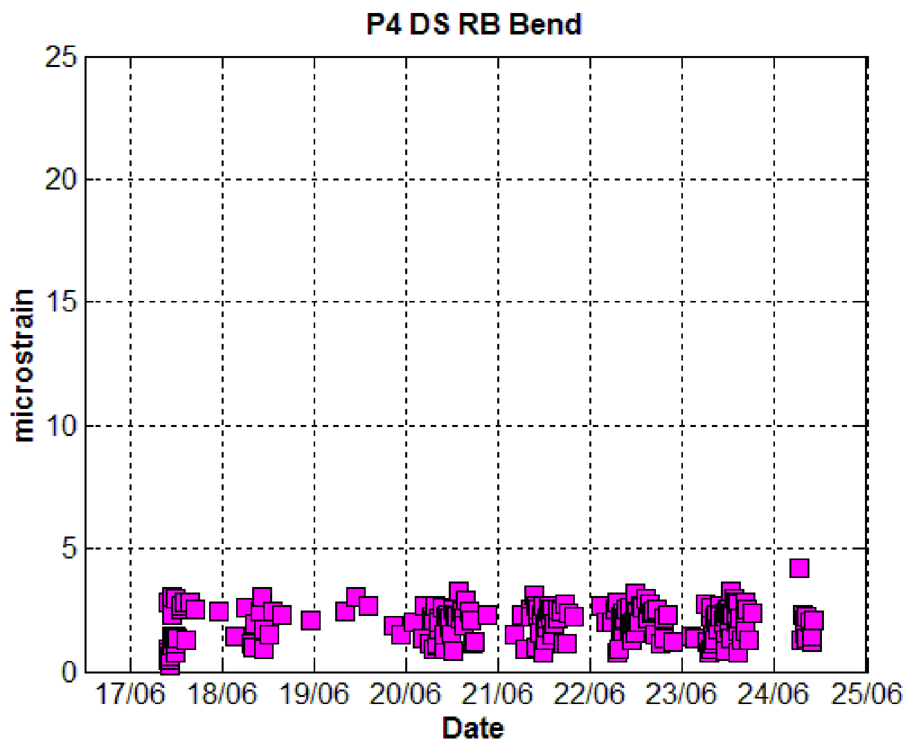

Figure 4-14. Scatter Plot - Pier 4 Downstream Bending Strain (RB)

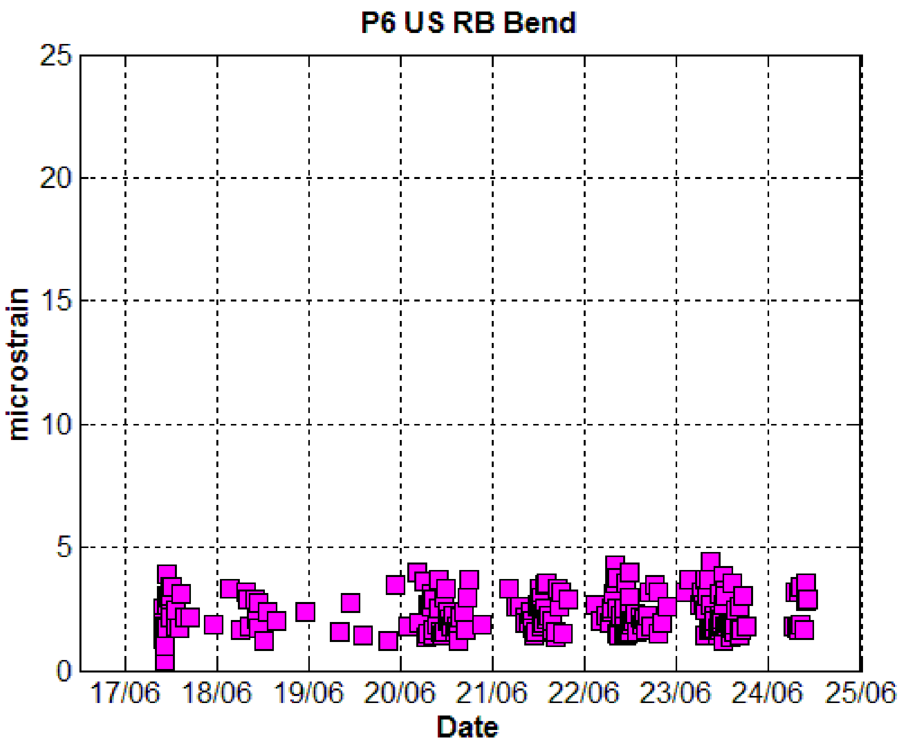

Figure 4-15. Scatter Plot - Pier 6 Upstream Bending Strain (RB)

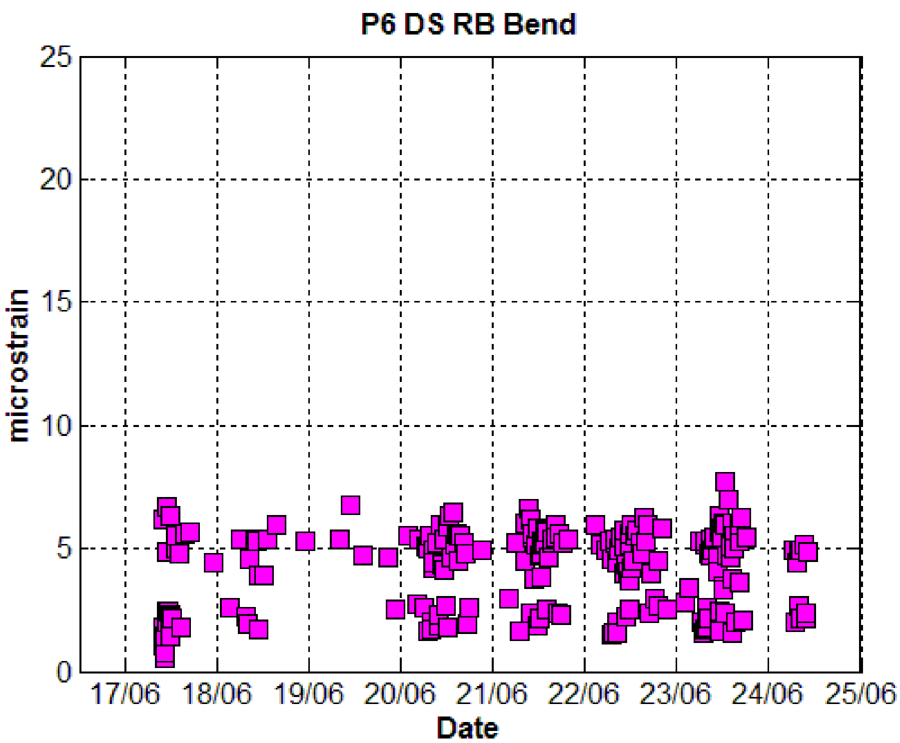

Figure 4-16. Scatter Plot - Pier 6 Downstream Bending Strain (RB)

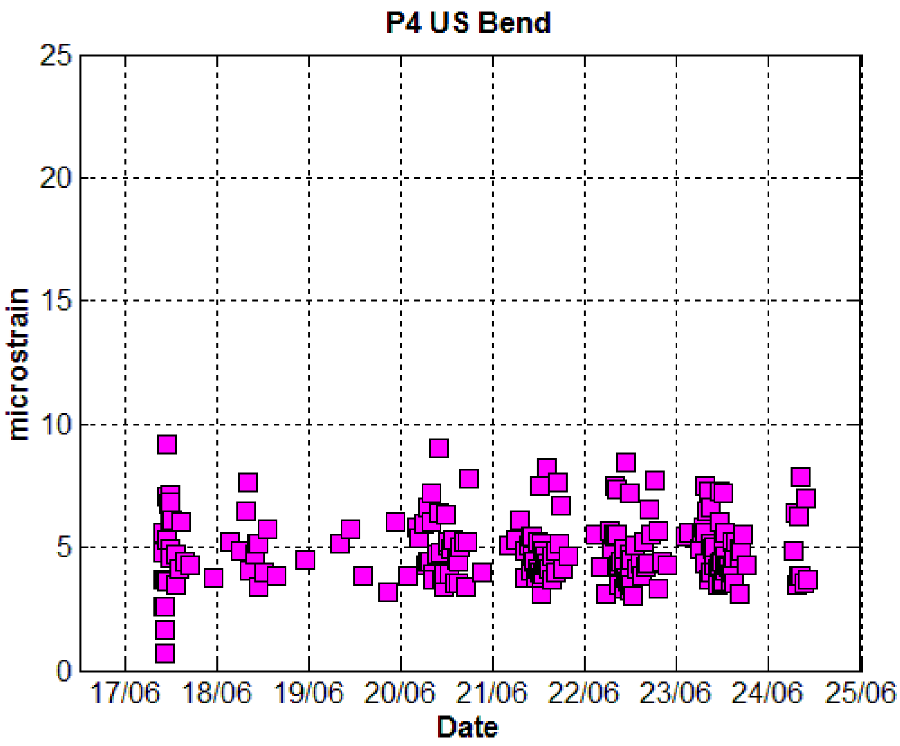

Figure 4-17. Scatter Plot - Pier 4 Upstream Bending Strain

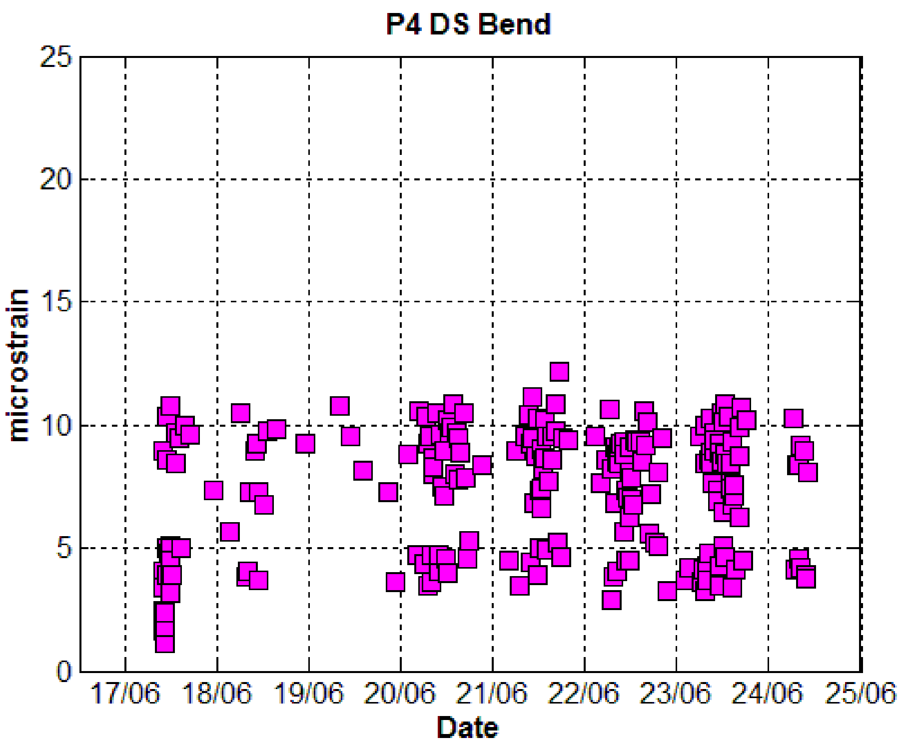

Figure 4-18. Scatter Plot - Pier 4 Downstream Bending Strain

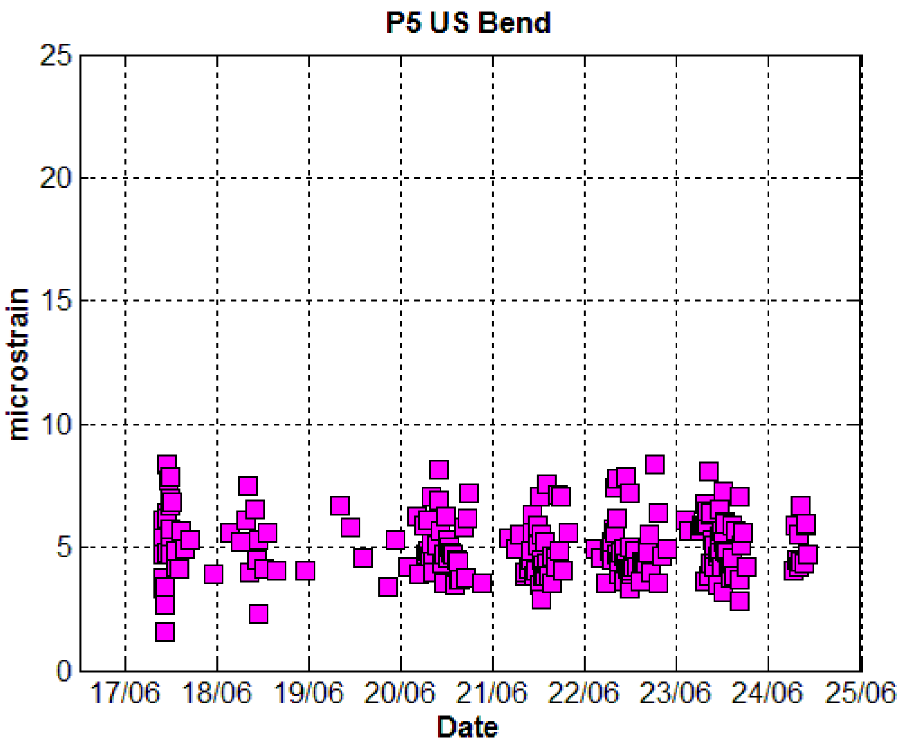

Figure 4-19. Scatter Plot - Pier 5 Upstream Bending Strain

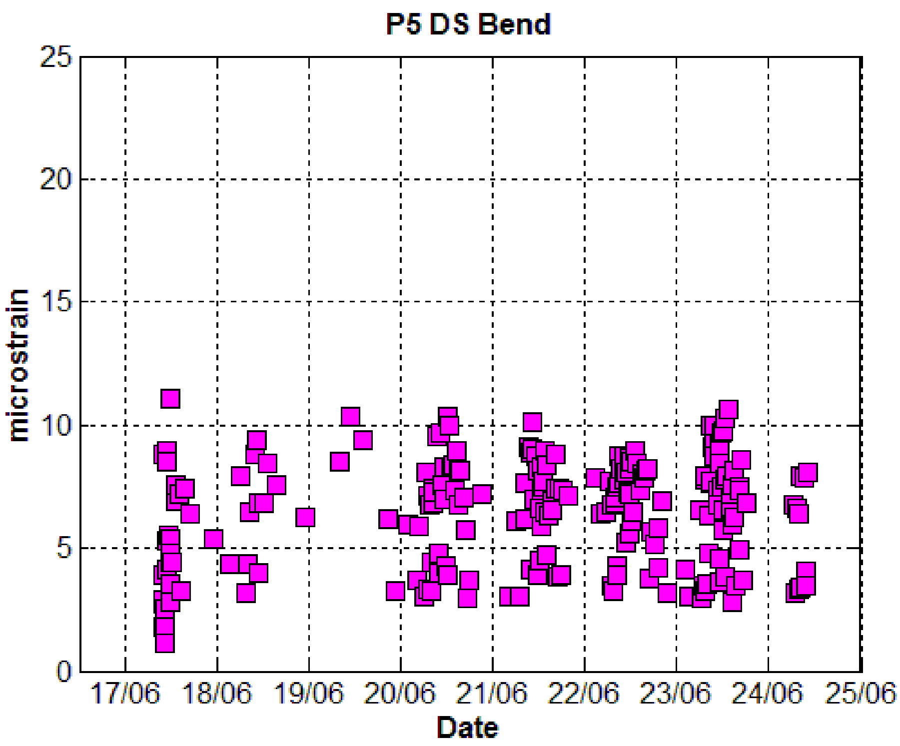

Figure 4-20. Scatter Plot - Pier 5 Downstream Bending Strain

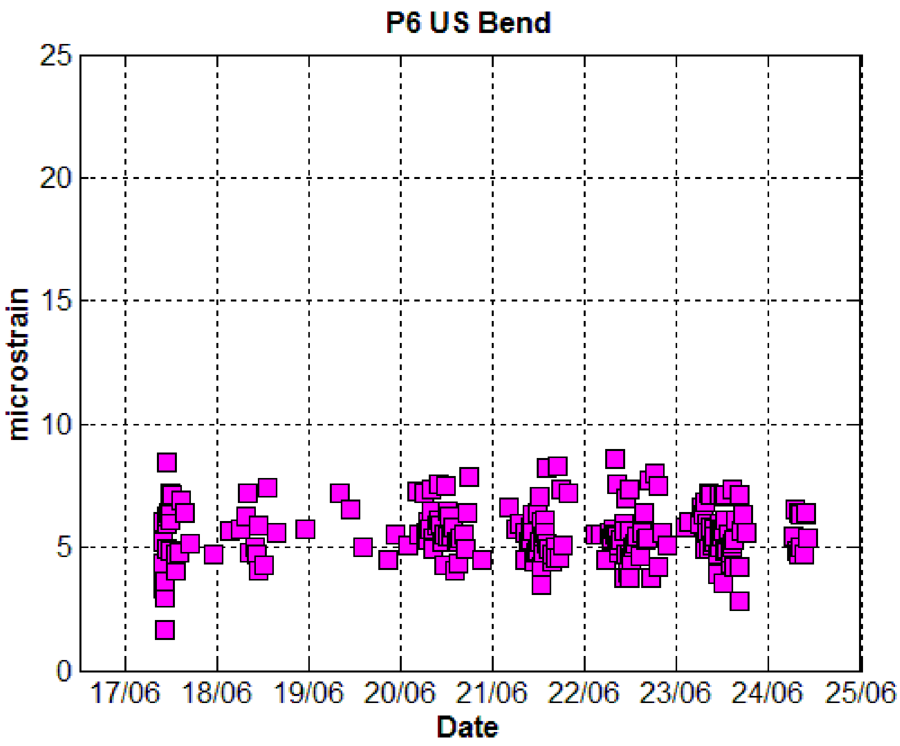

Figure 4-21. Scatter Plot - Pier 6 Upstream Bending Strain

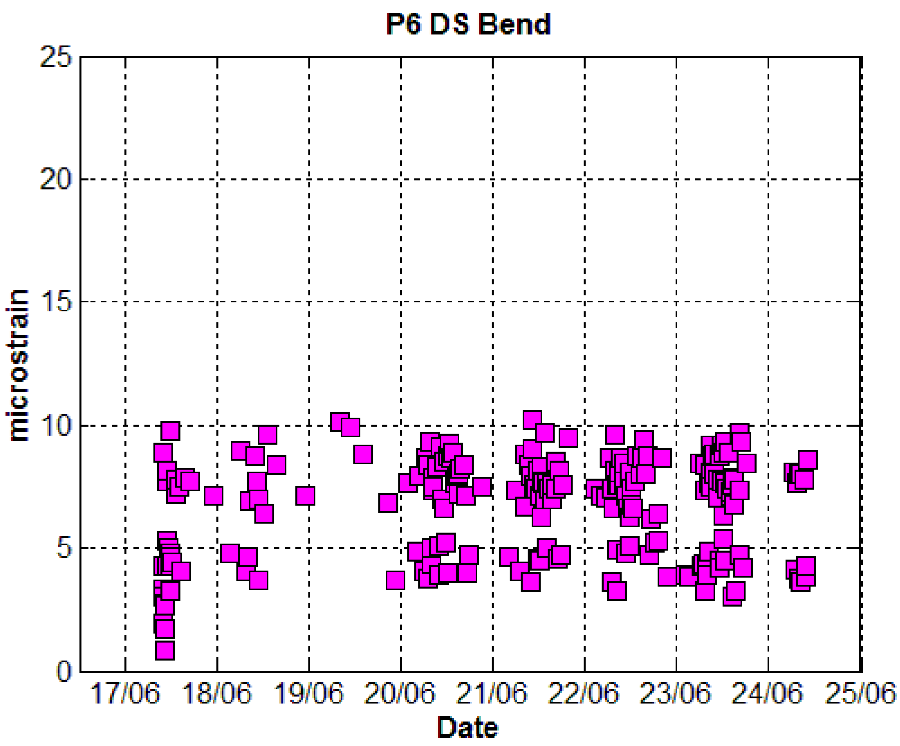

Figure 4-22. Scatter Plot - Pier 6 Downstream Bending Strain

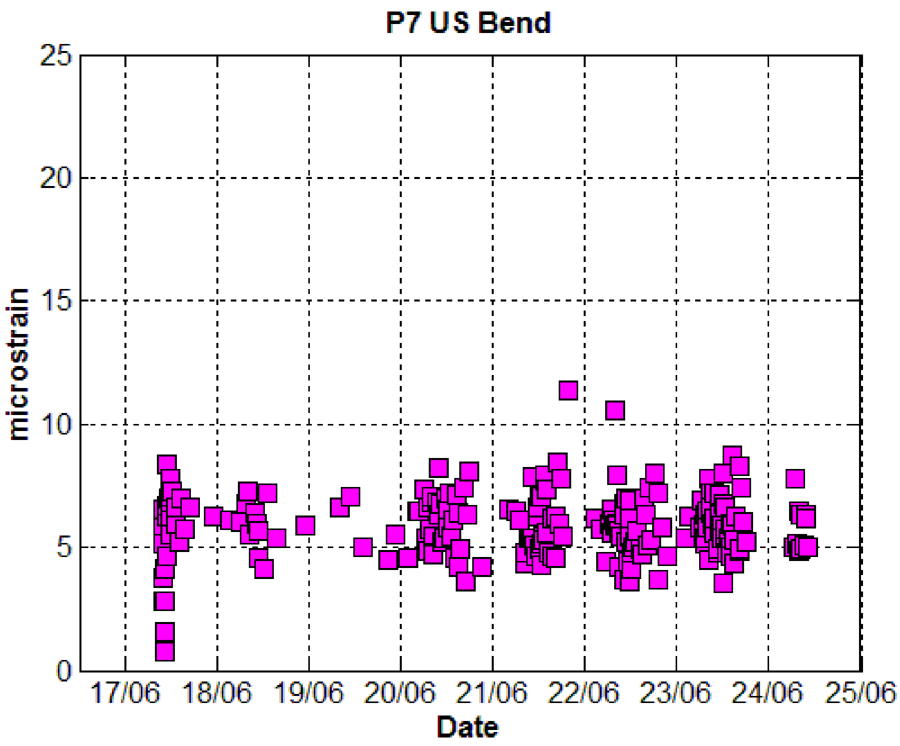

Figure 4-23. Scatter Plot - Pier 7 Upstream Bending Strain

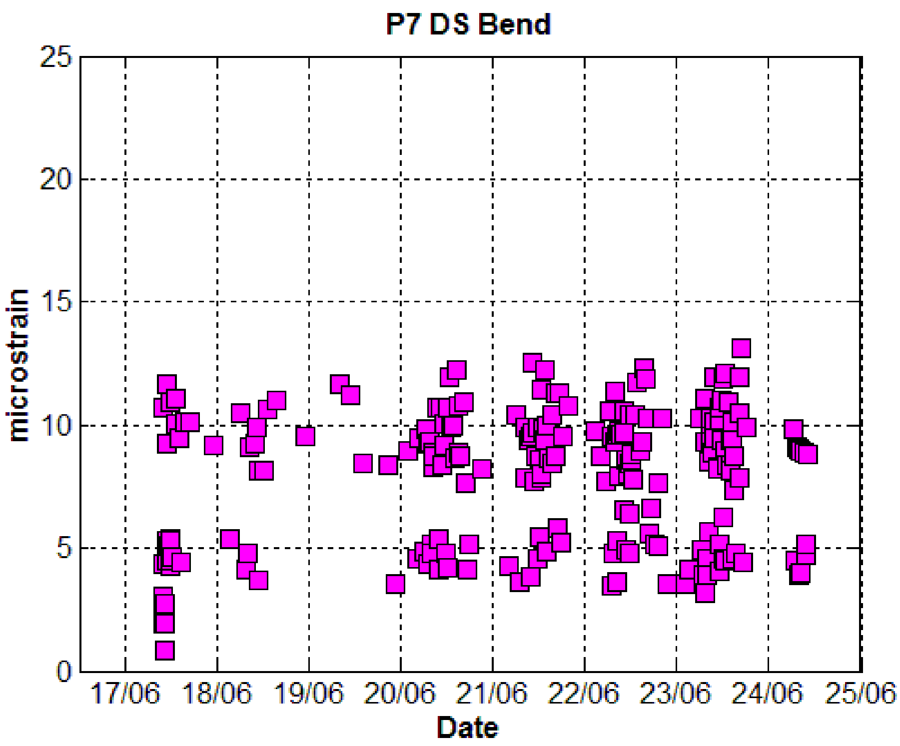

Figure 4-24. Scatter Plot - Pier 7 Downstream Bending Strain

5. Figures

Figure 5-1. Data Acquisition Location

Figure 5-2. Strap-On Strain Gauge for River Bed

Figure 5-3. Typical Pier Cabling

Figure 5-4. Expansion Joint DDT

CTI Consultants Pty Ltd

Head Office:
4 Rothwell Avenue,
Concord West NSW 2138

ABN 56 003 824 815
PO Box 153,
North Strathfield NSW 2137

www.cticonsultants.com.au
P: (02) 9736 3911
F: (02) 9736 3287

Graphitisation Investigation

Windsor Bridge

Prepared for: Roads & Traffic Authority NSW 110 George St Parramatta NSW 2150		**Contact:** Peter Ton **Phone:** (02) 8837 0843 **Mob:** (0407 295 624
Date: July 13th, 2011	**Job Number:** 2739	**Report Number:** C11231 **Rev:** 0riginal

Report No. C11231

Issued by

Fred Salome, B.Sc. (Hons.)
ACA Corrosion Technologist
NACE Certified Coating Inspector

Director
CTI Consultants Pty Ltd
(ABN 56 003 824 815)

4 Rothwell Avenue, Concord West NSW 2138 Australia
PO Box 153, Nth Strathfield NSW 2137 Australia
Telephone (02) 9736 3911 Facsimile (02) 9736 3287

e-mail: fred@cticonsultants.com.au

Revision	Date	Reason for Revision	Approved By
0	13/07/2011	Original issue	F. Salome

Disclaimer

TABLE OF CONTENTS

1 INTRODUCTION

As part of its ongoing asset management program, the Roads and Traffic Authority of NSW (RTA) has been gathering data on the condition of its bridge structures.

Many older bridges have cast iron piers[1] footed in rivers or estuaries and over recent years, concerns have been raised about the condition of many of these structures. One of the main concerns is the possibility of graphitisation of the cast iron piers, especially in the splash and tidal zones in coastal environments.

CTI Consultants have been providing assistance to the RTA in the assessment of graphitisation of cast-iron bridge piers since 1999, and have previously carried out graphitisation surveys on cast iron bridge columns of a number of bridges including the Unwins Bridge and Undercliff Bridge over the Cooks River at Tempe, the Pacific Highway Bridge over Wyong Creek, the old truss bridge over the Shoalhaven River (Nowra Bridge) at Nowra and the Bridge over the Patterson River at Hinton.

The results of the previous surveys showed that, in general, the extent of graphitisation was surprisingly low in the tidal and splash zone, but that graphitisation in the immersed sections of piers was considerably more advanced, with depths of graphitisation up to 25 mm being reported even in brackish and fresh water conditions.

CTI conducted a previous study on the columns of the Windsor Bridge on the Hawkesbury River in 2005, the findings of which were reported in CTI Report C10174, dated 30/04/2005. Based on a limited, random core sampling program, this investigation revealed high rates of graphitisation, with residual wall thickness being as low as 12 mm in places. This investigation also raised uncertainty about the original design thickness of the column castings, thought to be 30 mm from available drawings, but with site observations suggesting a 25 mm wall thickness.

In order to gain a more thorough understanding of the dimensions and wall thickness of the cast-iron column segments at Windsor (and other bridges), CTI proposed an additional program of core sampling, involving eight cores to be taken from the same segment, four cores at the cardinal points at both the upper and lower quarter circumferences. The divers would first be asked to identify the seams between the individual castings by cleaning a strip approximately 200 mm wide down the side of the selected column. This would allow the length of the segments to be established.

This report contains the details and findings of the latest investigation into the condition of the cast-iron piers of the bridge at Windsor. Although a stand-alone report, the reader is referred to the previous CTI Reports (C9666, C9880 and C10174) which contain background information on the composition, strength and corrosion of cast iron bridge piers as well as the above-water and under-water findings for the other bridges mentioned above.

[1] The cast iron columns of these piers are usually filled with concrete or rubble, but the iron casing provides the principal load bearing function.

2 METHODOLOGY

2.1 Details of Survey

The survey was conducted over the period from Monday, May 9th, 2011 to Saturday, May 21st, 2011.

All underwater work and inspections were provided by Commercial Diving Solutions Pty Ltd of Sapphire, NSW, (Manager Martin Woschitzka) under the on-site direction of Mr John Selway of the RTA Hunter Region. The inspection work was to coincide with the installation of other instrumentation on the bridge, directed by Mr Peter Ton of the RTA Bridge Section.

Fred Salome of CTI attended site at regular intervals to brief the divers on the requirements of the cleaning and core sampling program, and to receive updated results and samples as these became available.

2.2 Site Nomenclature

The bridge is oriented in an essentially NS direction. The piers are numbered from the south. Columns are denoted as D – Downstream or U - Upstream

The divers adopted a convention of referring to the upstream (West) direction as 12 o'clock, and working in a clockwise direction from there so that North is 3 o'clock and so on.

All reported heights on the piers were measured from a reference level corresponding to the lower of the two flanges on the columns.

The water level varied between approximately 2 and 3 m below the reference height, and the river bed was at approximately 8 m below the reference height (ie 5 to 6 m deep) for most of the river's width.

View of above water part of bridge pier showing lower flange used as reference level for recording height on piers

2.3 Inspection Procedures

2.3.1 Pre-Inspection

Before carrying out any cleaning tasks, the divers inspected the columns for visual signs of corrosion, noting the prevalence of marine growth, instances of loose rust tubercules and the relative incidence of hard nodules.

2.3.2 Cleaning

Vertical strips of approximately 150 mm width were cleared (using scraping and high pressure water) on target columns. The main purpose of this was to identify the seams between the individual castings comprising the columns, but this also allowed the columns to be checked for horizontal (circumferential) cracks.

Where cracks were encountered on any column, the entire circumference was cleaned.

2.3.3 Depth of Graphitisation

Cleaned areas were explored for depth of graphitisation by focussed application of the high pressure water nozzle or by probing with a chisel. The pins of a profile gauge were pushed into the excavated graphite layer to indicate its thickness, and photographed. This allowed the range of metal loss (= depth of graphitisation) to be determined.

2.3.4 Wall Thickness

Small diameter (20 mm) core samples were taken through the wall of the columns at selected locations, to allow the residual wall thickness to be measured directly. Where the graphite layer remained on the core undisturbed, the original total wall thickness could also be deduced (assuming no loss of graphite had occurred under service conditions, see discussion below).

2.4 Analysis of Water

Water samples were taken by the divers from near the surface, at mid-depth and close to the sea-bed.

CTI forwarded these samples to Envirolab Services of Chatswood, NSW, for analysis of a range of water quality parameters as further described in the results section below.

2.5 Metallurgical Examination

One sample taken from the lowest segment of Pier 5 visible above the sea-floor was examined metallurgically, for comparison with samples analysed as part of the 2005 survey.

2.5.1 Sample Preparation

The core samples was mounted and polished, and the microstructure viewed under a metallurgical microscope both in the un-etched and etched condition.

The un-etched condition was viewed at 120X magnification to identify the type of cast iron and to indicate the size, shape and distribution of the graphite phases.

To obtain an indication of the composition of the iron matrix, the samples were etched in 3% Nital and viewed at 250X magnification.

2.5.2 Hardness Testing

A Vickers Hardness test, using a 20 kg load, was performed on the cast iron sample to obtain an indication of the tensile and compressive properties of the material.

In cast irons, the strength is determined by the size and distribution of the graphite flakes and the composition of the matrix. The lower grades of cast iron tend to have a fully ferritic softer matrix compared to a fully pearlitic harder matrix for the higher strength grades.

2.5.3 Chemical Composition

Part of the sample was sent to Spectrometer Services for elemental composition analysis by electric arc spectroscopy.

3 RESULTS

3.1 Description

The piers are footed in the river-bed which is approximately 5m deep.

There is diagonal bracing in the atmospheric zone with a tie-beam located at approximately the low water mark, as indicated in Figure 1. The tidal range is of the order of 1 metre.

Note that the cross bracing at present is fixed to the columns by means of cleats at the top, with the cleats having been riveted onto the cast iron columns. However at the base, the bracing is secured by means of collars clamped around the columns, at the bottom of the tidal range (see arrows in Figure 1).

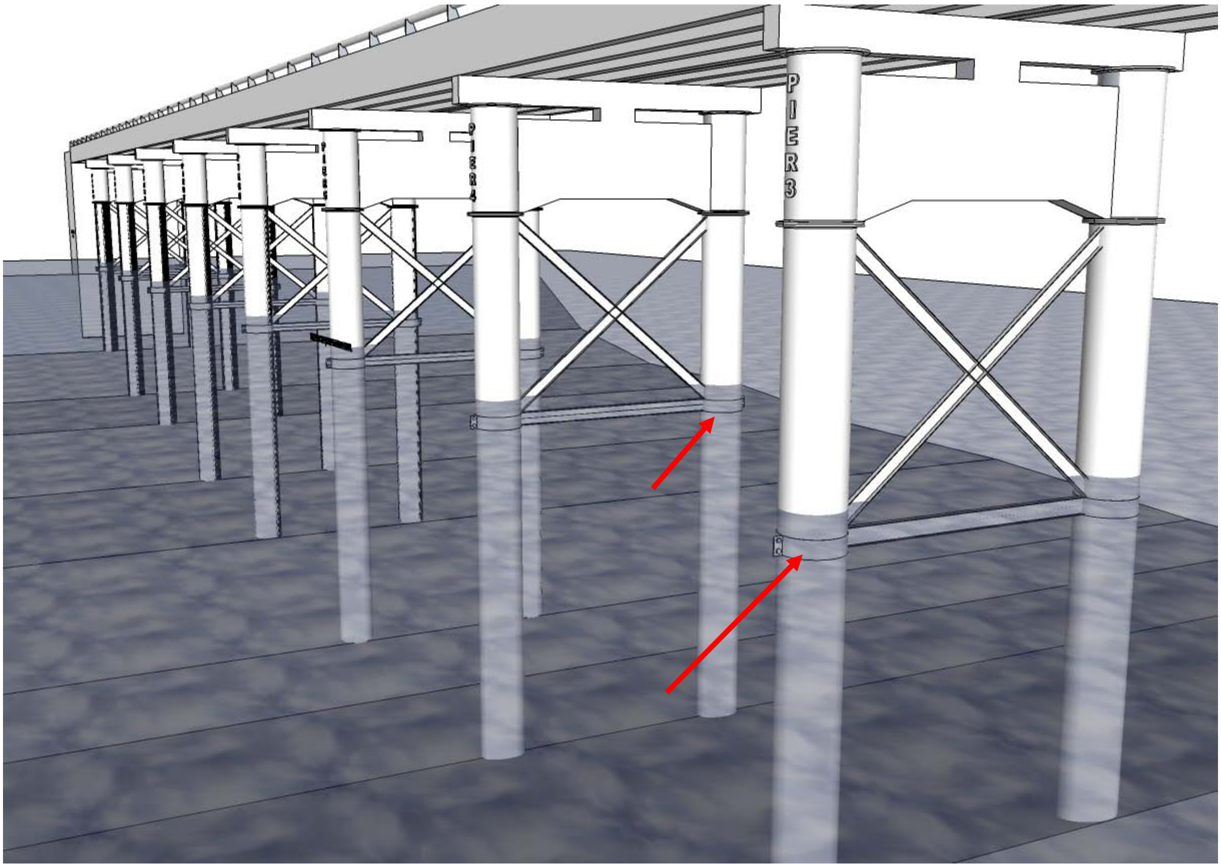

Figure 1 Sketch Showing General Arrangement of Piers

3.2 Design of Castings

After performing the strip cleaning of each pier, the individual castings were found to be 1.84 m in height (ie. 6 feet).

Core sampling into one of the seams (Pier 5 Downstream, mid-water level) revealed there to be an internal flange, with a bolt hole intersected by the core as indicated by the concave shape at its end. This confirms the castings are joined by internally bolted flanges.

	
Core from seam between sections as retrieved by divers - length > 50mm, with cast-in rebate for gasket (two halves taped together)	Inner ends of the two halves of the core were a concave shape, indicating the core intersected a bolt hole

3.3 Wall Thickness

3.3.1 Original Thickness

Core sampling of one casting (on pier 5) was conducted on two circumferences, at the upper and lower quarters, with samples taken at four equidistant points on each circumference (NW, NE, etc). The graphite layer on the core samples was largely undisturbed during the coring so that the total original wall thickness could be measured.

The results are presented in Table 1, which also includes the results from the 2005 survey. Together these indicate that the castings were made with a wall thickness ranging from 22 to 38 mm, but with most samples falling between 22mm and 29mm.

The results are considerably lower than found for the above water extension castings in 2005 and are lower than the indications on drawing which suggested a 30 mm wall thickness.

However, a core was taken from the base of column 5D, as the divers reported the surface condition before cleaning to be significantly different, with fewer and smaller tubercules or lumps in the marine growth layer. The length of this core was only 22mm, but it had only minimal graphitisation, less than 1 mm.

Metallurgical assessment of this core (refer section 3.6 below) confirmed it to be of the same type and composition as the remainder of the castings, as determined as part of the 2005 survey.

As it is considered highly unlikely that a lower wall thickness would have been used at the base of the columns, it is concluded that the original thickness was indeed greater than 22 mm, and that the graphitised layer has been worn away.

Scouring or sediment (essentially sand) loading at the base of a column during periods of high flow might be assumed to be significant and can provide a possible mechanism for the gradual erosion of the graphitised layer.

Another possible cause of loss of the marine growth or graphitised layers is prior cleaning and assessment. A thorough search of available records may provide further information on the likelihood of this having occurred.

Core from base of 5D, total length 22mm

Surface of core showing minimal (< 1 mm) graphitisation

3.3.2 Remaining Thickness

The remaining effective wall thickness (ie. exclusive of graphitised material) as measured during May 2011 ranges widely, from a maximum of 27 mm to a low of 2 mm.

There was no distinct or discernible pattern to the distribution of the residual wall thickness.

It should be noted that in addition to the core samples taken, the divers also measured the depth of graphitisation by excavating through the graphitised layer. This frequently showed depths of graphitisation in excess of 20mm, so that the residual cast iron thickness will be less than 10 mm and perhaps, in some instances, negligible.

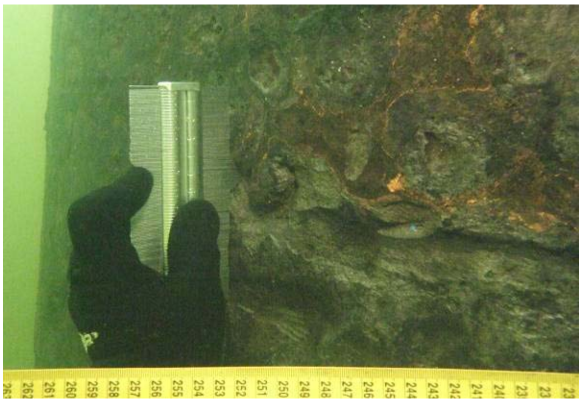 Measuring depth of graphitisation – diver pushing pins of profile gauge into excavation through graphite layer	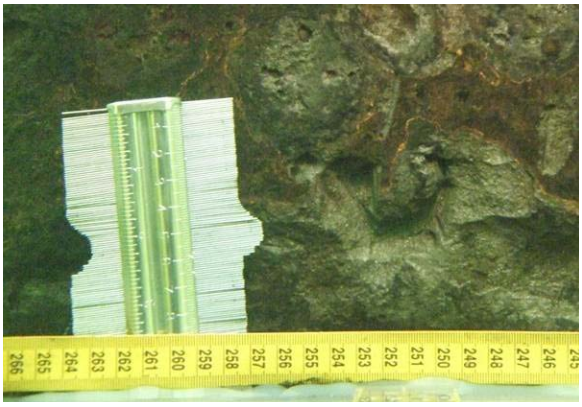 Profile gauge withdrawn from excavation allows depth of graphitisation to be measured
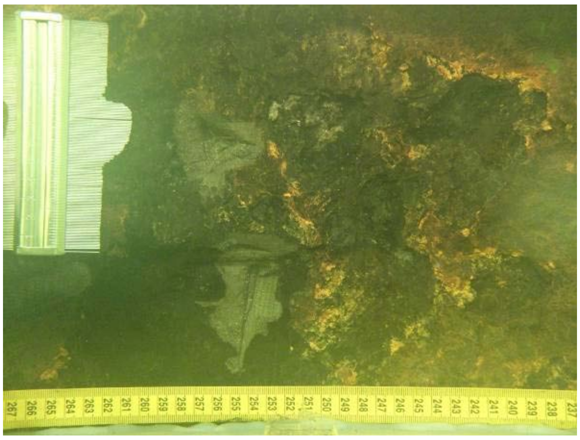 Profile gauge withdrawn from excavation allows depth of graphitisation to be measured	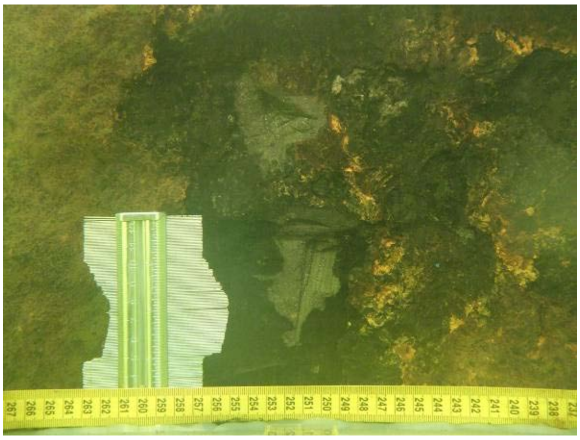 Profile gauge withdrawn from excavation allows depth of graphitisation to be measured

Table 1 Summary of Core Samples (2005 and 2011)

Date Cored	Pier	Column	Aspect	Height	Casting Length	Residual Cast Iron	Comment
Above Water							
10/03/2005	1	D		Above water, above flange	35	35	Column extension
10/03/2005	1	D		300mm below flange	26	26	Upper limit of immersed column sections
May 2011	5	D		Ref less 2m	26	26	Above MHWS
May 2011	5	D		Ref less 2m	23	23	Above MHWS
May 2011	5	D		Ref less 2m	25	25	Above MHWS
May 2011	5	D		Ref less 2m	26	23	Above MHWS
Below Water							
10/03/2005	1	D		1600mm below flange	25	25	
11/03/2005	5	D		Underwater	31	> 20	At internal thickening
11/03/2005	5	D		Underwater	~30	20	1.6m from bed
11/03/2005	7	D		Underwater	~ 38	18	1.6m from bed
11/03/2005	9	U		Underwater	~38	27	1.6m from bed
May 2011	5	U	NW	Ref less 4m	22	6-10	~ 0.7m below water
May 2011	5	U	NE	Ref less 4m	24	14-15	~ 0.7m below water
May 2011	5	U	SE	Ref less 4m	24	10-11	~ 0.7m below water
May 2011	5	U	SW	Ref less 4m	22-23	8-13	~ 0.7m below water
May 2011	5	U	SW	Ref less 4m	22-23	2-9	~ 0.7m below water
May 2011	5	U	NW	Ref less 5m	22	14-17	~ 1.7m below water
May 2011	5	U	NE	Ref less 5m	29	21-27	~ 1.7m below water
May 2011	5	U	SE	Ref less 5m	~28	18-20	~ 1.7m below water
May 2011	5	U	SW	Ref less 5m	27	16-21	~ 1.7m below water
May 2011	5	D		Ref less 3.6 m	23	11	50mm core through crack
May 2011	5	U		Ref less 3.35 m	27	15-17	50mm core through crack
May 2011	5	D		Ref less 8m	22	21	Sea-Bed core

Typical appearance of cores is illustrated in the following photographs.

 5D NE aspect, above water; no graphitisation	 5U NE aspect, upper quarter of immersed casting, showing 9-10mm of graphitisation and 14-15mm remaining cast iron
 5U SW aspect, upper quarter of immersed casting, showing up to 18 mm of graphitisation and as little as 2mm remaining cast iron	 5U SW aspect, lower quarter of immersed casting, showing up to 11 mm of graphitisation and as little as 16mm remaining cast iron

3.4 Cracking in Columns

During the inspection, three horizontal (circumferential) cracks were detected in columns.

The Upstream Column of Pier 5 (5U) had a full circumferential crack, approximately 200mm above the seam at the top of first fully immersed section. This placed the crack just below the collar for the bracing, and it probably coincides with the beginning of the internal thickening of the casting to create the flange. The crack was at its widest on the downstream (6 o'clock) side of the pier, where it was estimated to be in excess of 1 mm.

There was also a vertical crack on the column, starting at the same seam (at 6 o'clock, east or downstream) and extending approximately 100 mm upwards. Its width was measured to be up to 2 mm wide at its base, tapering upwards.

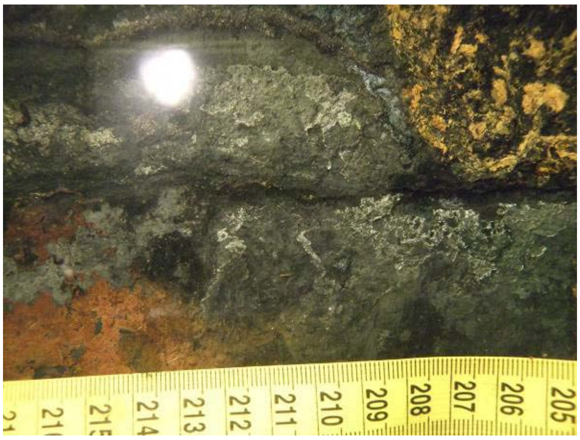 Circumferential crack on column 5U	 Circumferential crack on column 5U
 Vertical cack on column 5U on downstream side, estimated to be > 2 mm wide at its base	 Cleaning and excavating graphite layer shows crack to extend beyond the outer graphite layer

The Downstream column of Pier 5 (5D) also had a full circumferential crack but in this case, the crack was approximately 200mm below the seam at the top of the first fully immersed casting. The crack was cored using a 50mm diameter bit, and confirmed the crack to be full depth. Graphitisation had followed the line of the crack for some distance, indicating the crack to be of some age.

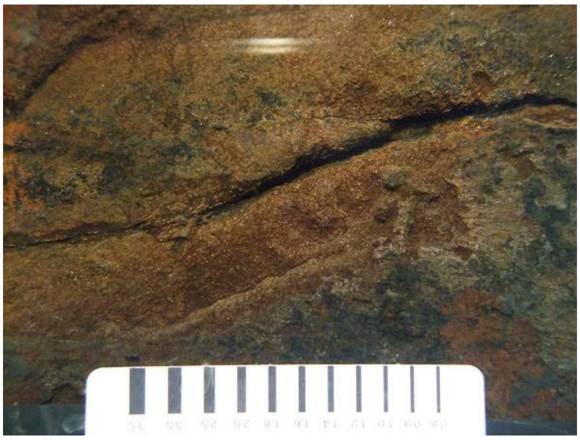 5D crack, at its widest on East, downstream side (6 o'clock)	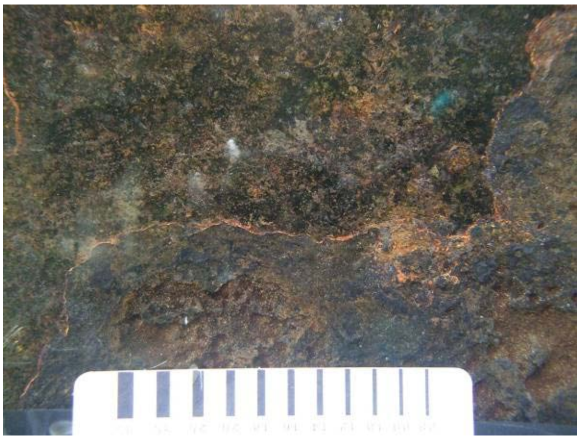 5D crack, narrow on West, upstream side (12 o'clock)
 Core (50mm diameter) through crack on 5D showing it to extend full depth through the casting	 Graphitisation follows line of crack indicating crack to be of reasonable age

The third circumferential crack was on the downstream column of pier 6 (6D), also situated below the first immersed seam, and extended for three quarters of the circumference, from 12 o'clock to 9 o'clock.

This crack was more complex, bifurcating at approximately 6 o'clock and developing parallel cracks for some distance. This suggests significant damage to the upper casing including the internal flange.

At its southern end (9 o'clock), the crack slanted upwards and joined the seam.

 Crack on 6D some 200mm below seam, with occasional frayed edges	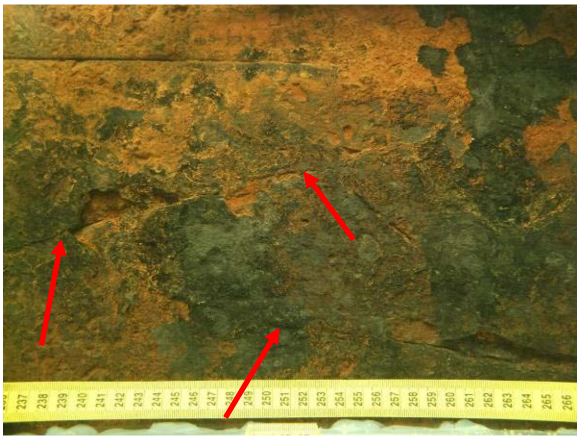 Crack bifurcates, indicating top of casting is essentially broken
 Twin cracks running parallel to each other	 Crack slants upward and joins seam at 9 o'clock (south aspect)

3.5 Water Quality

The results of the river water analyses are presented in Table 2.

Table 2 River Water Analysis Results

Test	CTI 38629 (Surface)	CTI 38630 (Mid depth, 2.5 m)	CTI 38631 (Bottom, 5 m)
Chloride (mg/L)	29	29	29
Sulphate (mg/L)	7	7	7
Electrical Conductivity (μS/cm)	170	170	170
Total Dissolved Solids (grav, mg/L)	86	100	96
pH	6.6	6.7	6.7
Hardness (mg$CaCO_3$/L)	24	25	23
Calcium (mg/L)	3.8	4.1	3.8
Iron (mg/L)	0.3	0.4	0.7
Potassium (mg/L)	2.0	2.2	2.0
Sodium (mg/L)	15	16	15

These results indicate that there has been no significant layering of the water, with no significant differences in any of the parameters tested. The water is essentially fresh water with a low hardness (soft).

The level of chloride and sodium present, at 29 ppm and 15 ppm respectively, are in fact well below potable water standards which have permissible chloride levels at 250 ppm and sodium at 180 ppm.

Therefore the waters sampled at Windsor Bridge during the survey indicate essentially fresh water with no marine influence. Although subject to tidal height water variations, this simply results in fresh water moving backwards and forwards by the pushing action of incoming tides, without sea water actually being present.

3.6 Metallurgical

3.6.1 Sample Details.

The cast iron core sample (CTI 38888) was taken by the divers at sea-bed level from the downstream Column of Pier 5 (5D) on 20/5/2011.

3.6.2 Microstructure and Hardness

The results of the metallurgical assessment are given in Table 3, which also reproduces the results for the earlier 2005 samples.

Table 3 Results of Metallurgical Tests and Estimates of Tensile Strength

Sample No.	Hardness (Hv_{20})	Microstructure	Estimated UTS*
CTI 25791	180 - 200	No evidence of graphitisation. Coarse flake graphite in fully pearlitic matrix plus relatively high levels of phosphide eutectoid (Figures 1 & 2 in 2005 Report)	220 to 240 MPa
CTI 25792	160 - 175	No evidence of graphitisation. Coarse flake graphite and fine rosette graphite in a ferritic/pearlitic matrix. relatively high levels of phosphide eutectoid (Figures 3 & 4 in 2005 Report)	180 to 200 MPa
CTI 25793	160 - 180	Graphitisation on outer surface. Coarse flake graphite in ferritic/pearlitic matrix plus relatively high levels of phosphide eutectoid (Figures 5 & 6 in 2005 Report)	180 to 200 MPa
CTI 25794	160 - 175	Graphitisation on outer surface. Coarse flake graphite and some rosettes of medium to fine graphite in a ferritic/pearlitic matrix plus medium levels of phosphide eutectoid (Figures 7 & 8 in 2005 Report)	180 to 200 MPa
CTI 25795	145 - 155	Graphitisation on outer surface. Coarse flake graphite and some rosettes of medium to fine graphite in a nearly fully ferritic matrix plus medium levels of phosphide eutectoid (Figures 9 & 10 in 2005 Report)	140 to 160 MPa
CTI 38888	160 - 175	Slight graphitization on outer surface. Coarse flake graphite and some rosettes of medium to fine graphite in a ferritic/pearlitic matrix plus relatively high levels of phosphide eutectoid (refer Figures 2 & 3)	180 to 200 MPa

* Based on shape and size of graphite flake, type of matrix and hardness.

The micrographs for the sample from 5D are shown below.

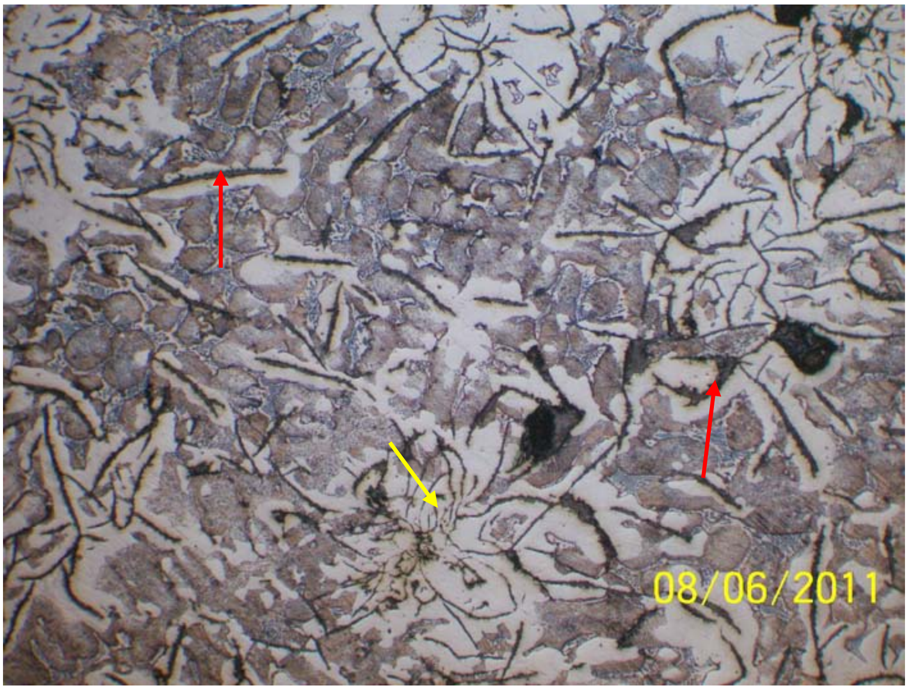

Figure 2 Core Sample CTI 38888 (etched) showing coarse graphite flakes (red arrow) and "rosettes" of medium and finer carbon flakes (yellow arrow) in a ferritic/pearlitic matrix. Magnification –X120; Etchant – 3% Nital.

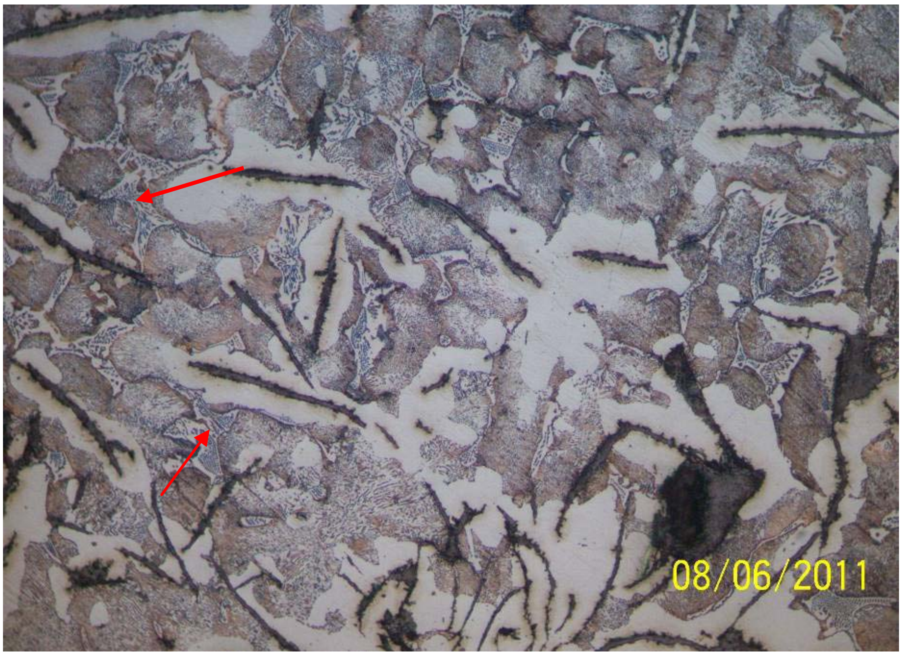

Figure 3 Core Sample CTI 38888 (etched) showing coarse and medium graphite flakes in a ferritic/pearlitic matrix containing relatively high levels of phosphide eutectoid (refer arrows). Magnification -X280; Etchant – 3% Nital.

3.6.3 Chemical Composition

The results of the chemical analysis are given in Table 4, which also reproduces the results for the earlier 2005 samples.

Table 4 Compositional Analysis

Sample	C (%)	Mn (%)	Si (%)	S (%)	P (%)	Ni (%)	Cr (%)	Cu (%)
CTI 25791	3.54	1.6	2.1	0.021	0.95	<0.01	<0.01	0.02
CTI 25792	3.16	0.66	2.6	0.048	1.2	<0.01	<0.01	0.01
CTI 25793	3.40	0.91	2.2	0.040	1.2	<0.01	<0.01	0.01
CTI 25794	3.15	0.76	2.4	0.075	1.4	<0.01	<0.01	<0.01
CTI 25795	3.16	0.69	2.70	0.060	1.1	<0.01	<0.01	0.01
CTI 38888	3.2	0.82	2.5	0.05	1.15	0.02	0.02	0.01

3.6.4 Discussion

The core sample from column 5D at sea-bed level was of grey cast iron as indicated by the presence of flake graphite. The size of the graphite flakes and the high level of phosphide eutectoid in the sample indicate the cast iron pier was relatively old and the tensile strength would be relatively low compared to modern day grey or SG iron.

There was no significant difference in chemical composition for the major elements although the nickel and chromium contents are very slightly higher in the sample from column 5D. The microstructure and hardness of the cast iron samples collected in 2005 and the sample from column 5D are similar.

4 DISCUSSION & CONCLUSIONS

4.1 Original Wall Thickness

The evidence from the two surveys to date indicates that the wall thickness of the immersed castings was of the order of 22 to 29 mm, say 25 mm on average.

This is based on the premise that no significant amount of the graphitised layer has been lost, so that the outer surface of the graphite represents the outer surface of the column at time of construction.

However there is now some reason to doubt this, with the core from the bottom of Column 5D having very little graphitisation and a total indicated wall thickness of only 22mm. As this is considered improbable, the above premise must be questioned.

It is now thought probable that erosion (at times of high river flow) has resulted in the marine growth layer and some of the graphitised layer being worn away, so that the original outline of the outer surface of the castings has, at least in some places, been irrecoverably lost.

4.2 Graphitisation

The condition of the columns as detected during the present survey reveals that graphitisation has advanced to significant proportions. Indications are that in places there is more than 20mm of graphitised material present.

There is no clear pattern to the extent of graphitisation, other than an apparent tendency for higher depth of graphitisation to occur on the upstream (West) side of the columns. This may be linked to debris disturbing the otherwise protective layer of marine growth, allowing more ready diffusion of oxygen to the corrosion front.

The high degree of graphitisation has occurred despite the river water at the bridge being essentially fresh, with no significant salt loading. It should be noted that evidence is emerging from other RTA bridges where cast-iron graphitisation in freshwater settings appears to be generally greater than for salt or brackish waters.

This phenomenon is being explored in a parallel report on graphitisation in other bridges in the Hunter and Northern regions.

4.3 Residual Wall Thickness

Residual cast iron (ie. effective wall thickness) varies but in places is very low, almost negligible. Bearing in mind the limited extent of the core survey, it is possible that full depth graphitisation may have occurred in places.

The average residual wall thickness from the underwater cores taken to date is approximately 15 mm, but the limited nature of the sampling suggests that a more conservative thickness should be used in any structural analysis.

4.4 Cracking

Horizontal cracking is present in three of the columns, including both columns in pier 5. They occur at quite shallow depths, and may be related to the location of the bracing collars just above where they occur.

There is also a short vertical crack on the upstream column of pier 5.

It appears that the cracks are not new and have been present for quite some time, at least a few decades and possibly longer.

Nevertheless such cracks would be expected to have a serious impact on the overall serviceability of the bridge, and a detailed structural analysis should be carried out to determine their probable impact on the bridge's capacity.

5 ADDITIONAL OBSERVATION

Although the scope of the investigation was limited to the underwater sections of the piers, it was noticed that on Pier 4, there are vertical cracks in the brackets securing the upper end of the diagonal bracing to the piles. Cracks are present in this bracket on both upstream and downstream columns.

The photograph below illustrates one of these cracks, on the downstream column of Pier 4. Note also that there is one bolt missing from this detail.

INSPECTION AND STRUCTURAL ASSESSMENT REPORT FOR

Bridge name:	Windsor Bridge
Location:	Bridge St, Windsor
Owner:	RTA
Date:	April 15, 2011
Report no:	C10-69-000-A

Authors:

Prof Bijan Samali
Mr Peter Brown

accessUTS Pty Limited
PO Box 123
Broadway NSW 2007 Australia
Tel +61 2 9514 1916 Fax +61 2 9514 1433

ABN 55 098 424 312

Report Authorised by:

Bijan Samali

Bijan Samali – access:UTS Consultant

TABLE OF CONTENTS:

PART ONE: SUMMARY OF OUTCOMES

1.1 Background to the Testing Program

The superstructure of Windsor Bridge was tested using Dynamic Frequency Analysis or DFA (as detailed in the Appendix A) to measure the global stiffness of the deck, in comparison to previous testing in 2003, to help establish the level of degradation to the superstructure's stiffness.

1.2 Brief Description of the bridge

The Windsor Bridge, which forms part of Bridge St. over Hawkesbury River in Windsor, NSW was built in 1874 and is a 7 meter wide, two lane carriageway and consists of eleven simply supported spans. The bridge deck is made of reinforced concrete slabs supported by eight concrete girders. Exact dimensions and design details were provided by the RTA of NSW.

PART TWO: INSPECTION PHASE

2.1 Background

The purpose of the bridge inspection was to determine any deterioration of structural condition, performance and capacity of the structure, measured by any changes to its flexural stiffness over the past seven years and to recommend appropriate management options. Inspection of the bridge components and an assessment of its condition were conducted according to the procedure and standard condition rating system as defined by Vicroads Bridge Inspection Manual (VBIM). The condition rating system reflects the performance, integrity and durability of the structure and its principal components.

The scope of the engineering inspection included:

- Detailed inspection of all bridge components, including testing and analyses as necessary to supplement visual inspection.
- Reporting on the condition, structural adequacy, evidence of distress, mode of deterioration, and projected deterioration.
- Recommendation of management actions and/or maintenance/rehabilitation treatment options.

For this bridge, however, the visual inspection was not comprehensive due to lack of adequate lighting at the time of testing and the fact that RTA of NSW had already performed such an inspection. Despite this, the visual inspection confirmed better overall conditions for spans 1 and 2 compared with spans 3 and 4.

PART THREE: FIELD TESTING PHASE

3.1 Introduction

An overview of the DFA procedure used in this project is presented below, with details of the instrumentation set-up and procedures for testing as noted in Appendix A. Graphs pertaining to field test results are presented in Appendix B.

This section presents a summary of the DFA results.

3.2 Flexural stiffness of the tested bridge

Table 3.1 shows the first natural frequency of each span tested and a relative span EI, compared to previously obtained EI of the subject bridge (span 1 only) by UTS in 2003, using DFA method.

The benchmark flexural (or bending) stiffness (EI) was calculated for span 1 from previous testing and using the recent measured natural frequency of span 1, a relative EI was calculated for that span. The governing equation is given below.

$$\omega = \sqrt{\frac{n * pi^2 * EI}{p * A * L^4}}$$

Where:

ω = natural frequency in rad/sec
n = mode number
EI = Stiffness
p = density of concrete
A =cross sectional area of tested span
L = span length

Table 3.1 - Results of relative stiffness using the proposed dynamic method

Span No.	First Natural Frequency (Hz)	Relative stiffness to previous testing
1 (2003)	12.5	100%
1 (2010)	11.4	84%
2	11.2	Not applicable
3	10.1	Not applicable
4	10.2	Not applicable

PART FOUR: CONCLUSIONS AND RECOMMENDATIONS

4.1 Assessment of the Bridge as Tested

The EI calculation, representing the bending stiffness of span 1, in comparison to previous testing, shows a drop in stiffness of 16% for span 1. It is not possible to establish the drop of bending stiffness for spans 2,3 and 4 as these spans were not tested in 2003.

The first flexural (bending) natural frequencies were obtained from relevant peaks in the Summation of Frequency Response Functions (FRF) graphs shown in Figures B.1 to B.4 in Appendix B for spans 1 to 4, respectively. Figure B.5 illustrates the Summation of FRF for Span 1 obtained in 2003. In this figure the relevant frequency is one for the span without added mass.

Based on these findings, it is clear that span 1 of the bridge has deteriorated over the past seven years by 16% and some load limits may have to be applied to slow down the rate of further deterioration. If the RTA intends to decommission the bridge in near future, the bridge in its present condition and loading will be safe for some time. However, if the RTA intends to maintain the bridge, further testing and employing parallel finite element analyses is recommended to translate this deterioration into a quantifiable load limit.

APPENDIX A –
Description of the Testing Procedures

A1 *Field Testing - Setup and Procedures*

Instrumentation

Accelerometers (piezo-resistive type) with high sensitivity and low frequency-range are installed on the superstructure to record the accelerations of the bridge deck. A large 12 lb Modally Tuned ICP Sledge Hammer is used to provide the excitation for the field tests along with a specially built drop mass sensor where higher excitation is required. A Computer based data acquisition system with 32 channel signal conditioners is used to record hammer force and acceleration response signals during the tests. Data processing, including Fast Fourier Transform (FFT) and Frequency Response Function (FRF) calculations are executed using a specifically developed MATLAB programme.

Test Setup

Accelerometers are mounted on the superstructure at mid span to monitor the vibration. Base plates are manufactured to allow the sensors to be bonded to the superstructure with minimal delays to traffic

Testing Procedure

The bridge 'as is', without additional mass, is impacted by the modal hammer or exciter at the centre of the carriage way at mid-span.

A2 *Data Processing and Analysis*

From recorded dynamic response time histories, using FFT, the auto spectrum of the given signal can be obtained. After auto spectra of the impact force and response of the bridge are obtained, the Frequency Response Functions can be computed. A computer programme has been developed using MATLAB software for this purpose. This software offers a great deal of flexibility when processing the test data. It produces the required Frequency Response Functions at a given bandwidth with good resolutions. Advanced Modal Analysis software, LMS CADA-X from LMS Company is also used in the analysis stage where highly nonlinear and coupled dynamic modes occur, for which normal peak picking method is no longer valid.

A3 *Dynamic properties of the tested bridge*

From the results of the modal analysis, dynamic properties of the tested bridge such as natural frequencies, damping ratio and mode shapes, can be obtained. However, the dynamic method requires only the first flexural natural frequency for subsequent analyses.

APPENDIX B –
Test Results

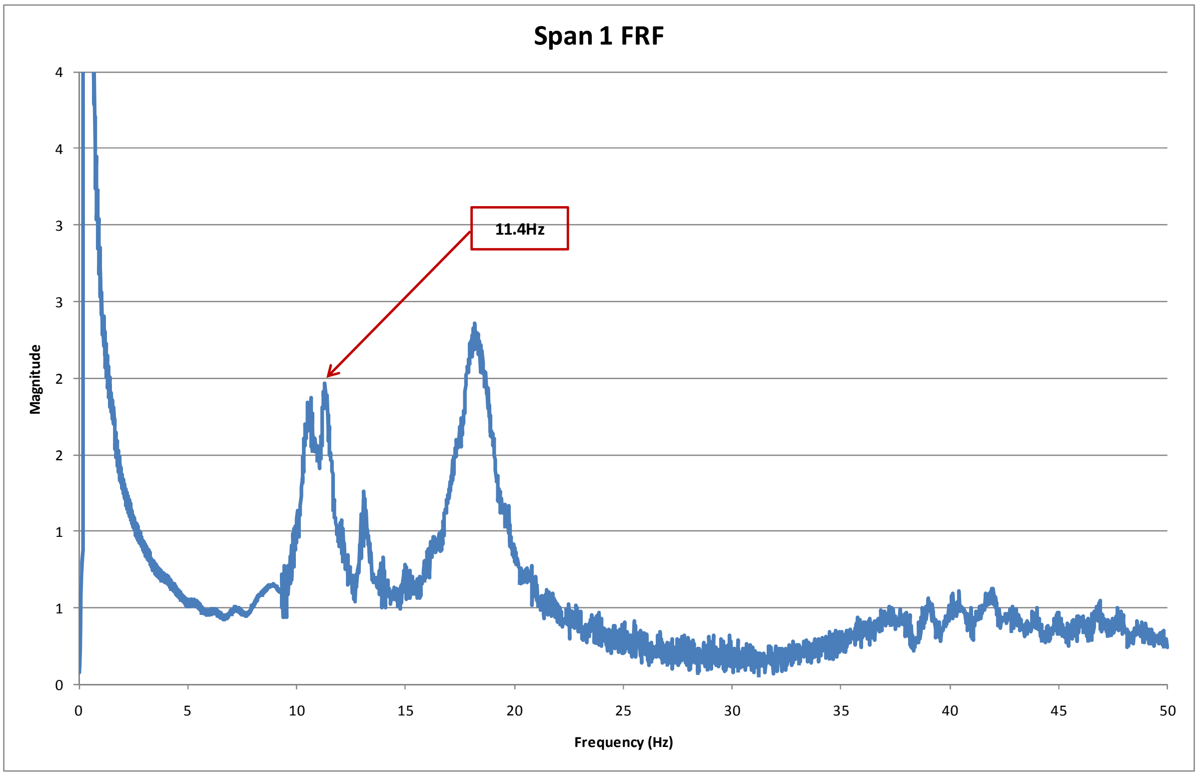

Figure B.1 Sum FRFs for span 1 of the subject bridge

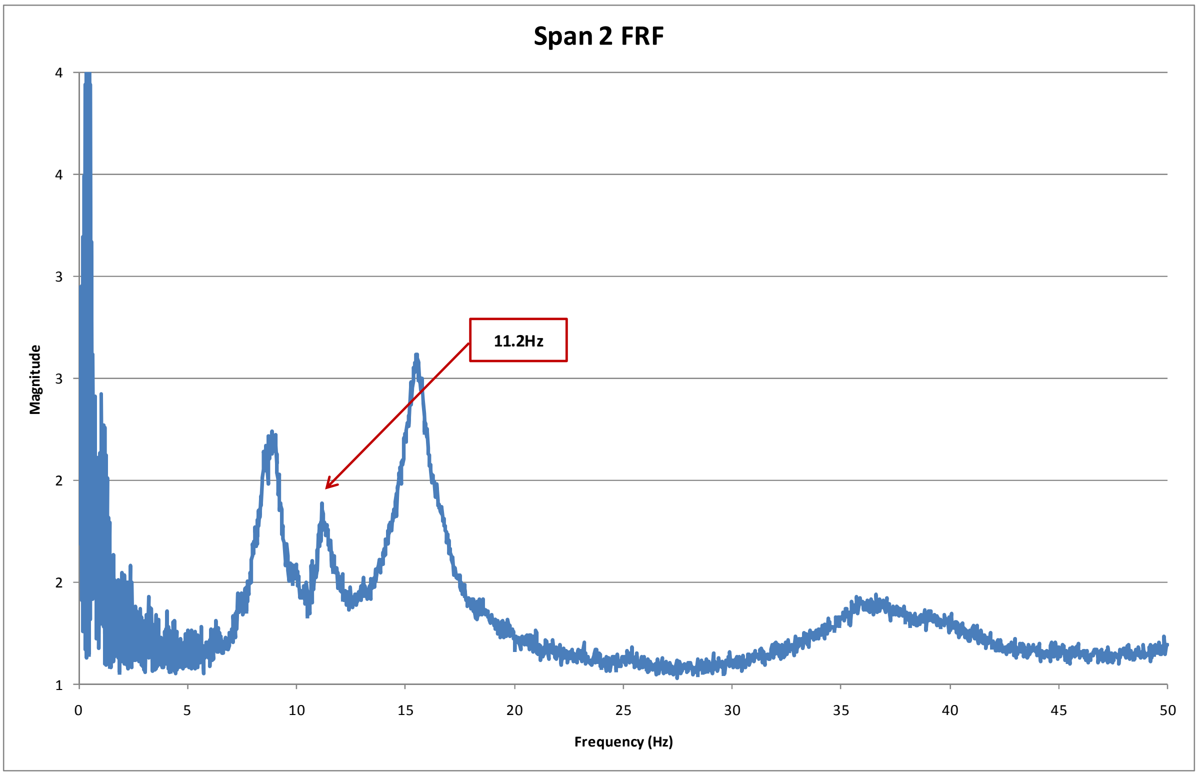

Figure B.2 Sum FRFs for span 2 of the subject bridge

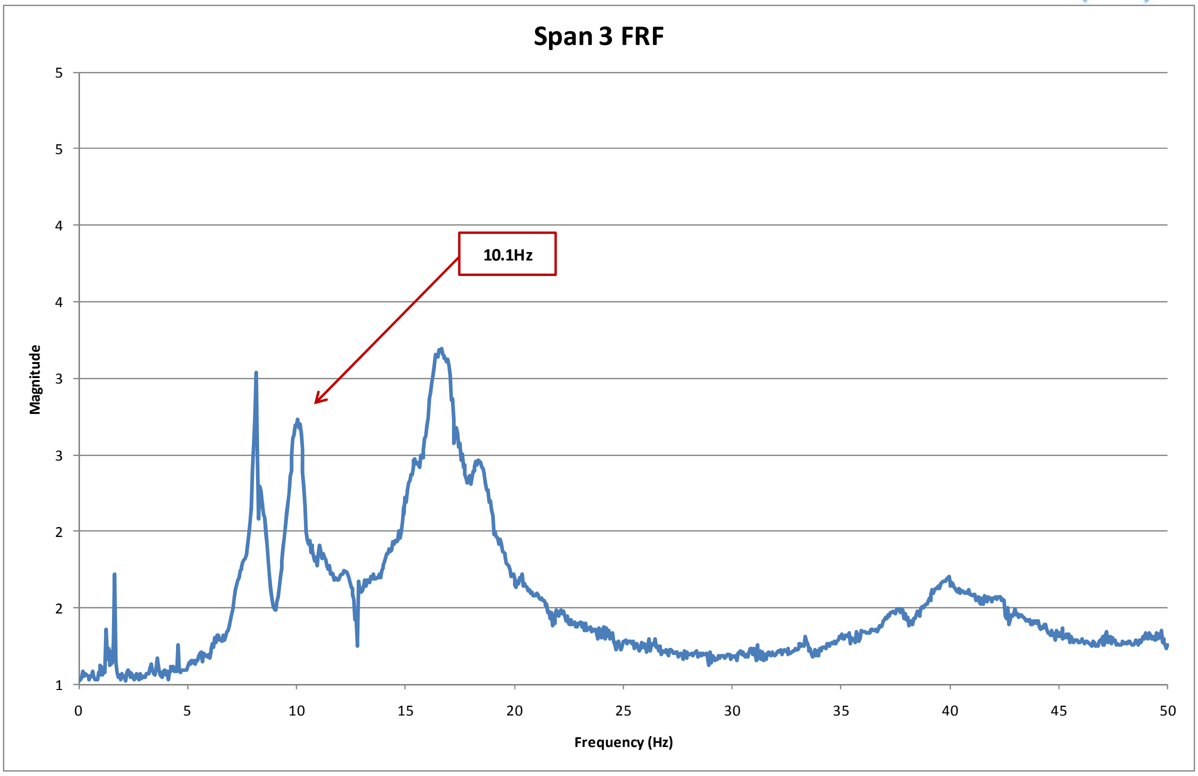

Figure B.3 Sum FRFs for span 3 of the subject bridge

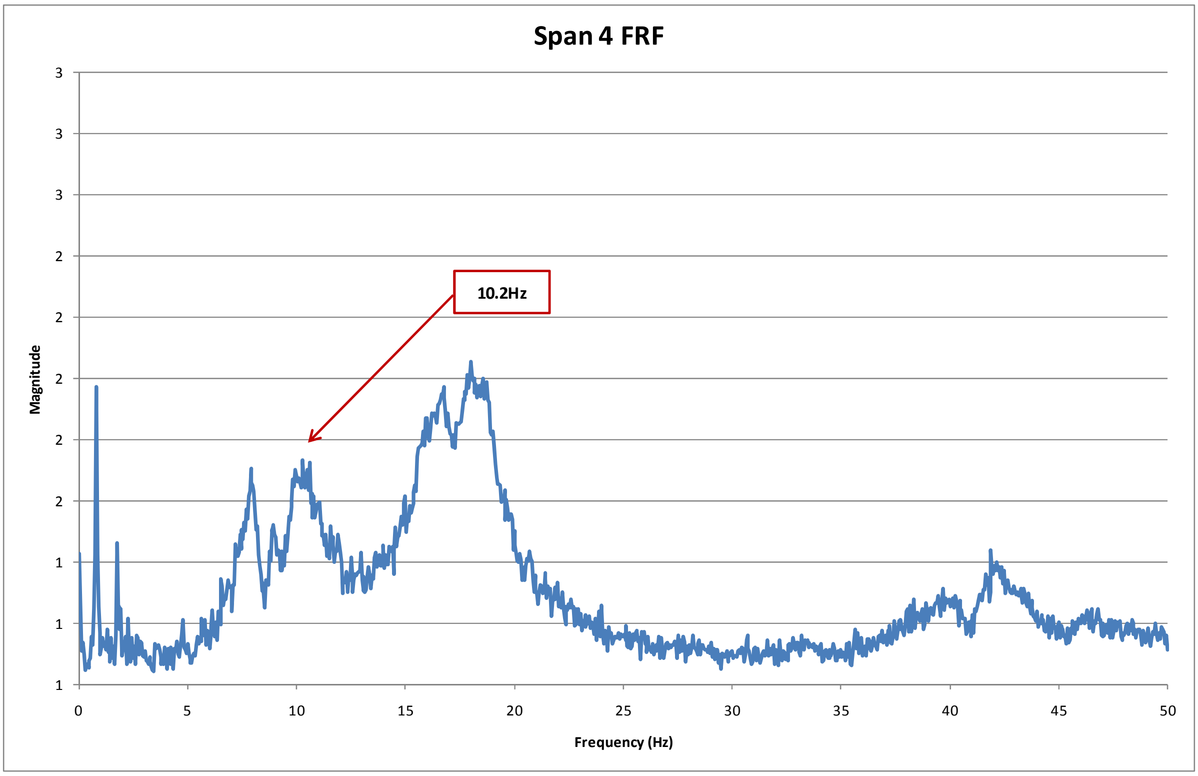

Figure B.4 Sum FRFs for span 4 of the subject bridge

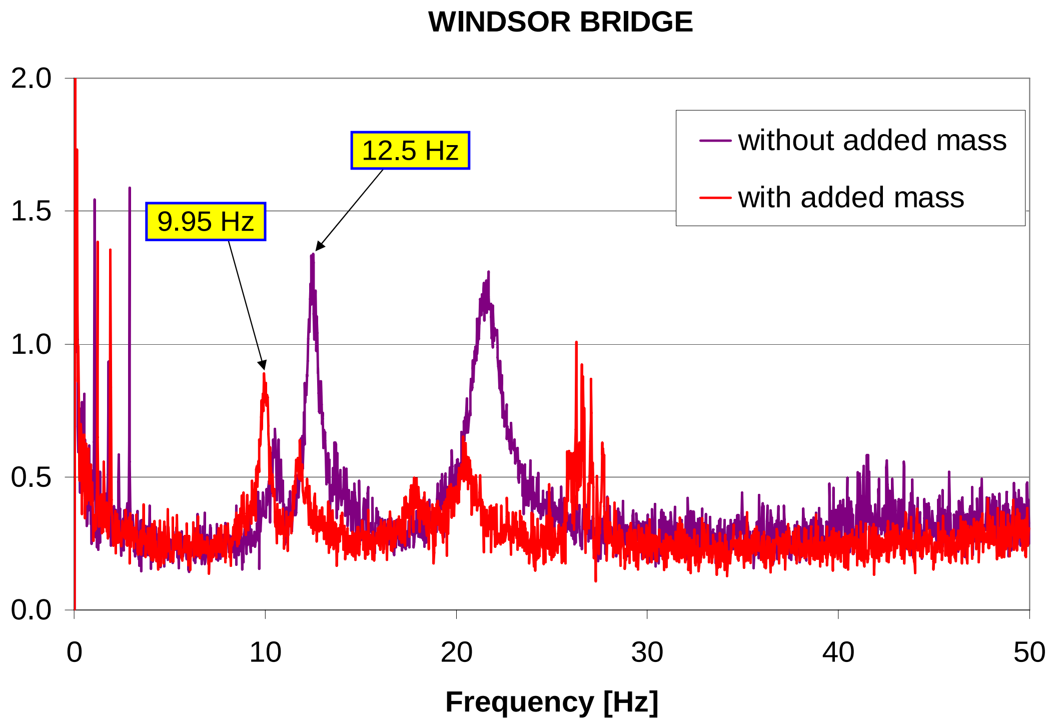

Figure B.5 - Sum FRFs for span 1 of Windsor Bridge with and without added mass in 2003